

Article

Simulations and Experiments of Soil Temperature Distribution after 2.45 GHz Long-Term Microwave Treatment

Xiaohe Sun ^{1,2,3} , Chunjiang Zhao ^{2,3}, Shuo Yang ^{1,3}, Haolin Ma ^{1,3} and Changyuan Zhai ^{1,3,*}

¹ Intelligent Equipment Research Center, Beijing Academy of Agriculture and Forestry Sciences, Beijing 100097, China; sunxh868@foxmail.com (X.S.); yangshuo@nercita.org.cn (S.Y.); ml262771854@163.com (H.M.)

² College of Resources and Environment, Jilin Agricultural University, Changchun 130118, China; zhaocj@nercita.org.cn

³ Information Technology Research Center, Beijing Academy of Agriculture and Forestry Sciences, Beijing 100097, China

* Correspondence: zhaicy@nercita.org.cn; Tel.: +86-135-1917-3503

Abstract: Soil disinfection is an important agronomic measure to prevent soil-borne diseases, insects, weeds and other hazards. Based on the premise of being environmentally friendly, microwave soil disinfection can improve crop yield and quality in a pollution-free, residue-free and green way. The law of microwave soil heating is the theoretical basis of microwave soil disinfection. Therefore, in this paper, loess soil of North China and black soil of Northeast China are used as test materials to explore the law of soil heating under the action of microwaves. First, COMSOL Multiphysics software was used to simulate the temperature field change in the microwave-irradiated soil, and a simulation model of the temperature field of the microwave-irradiated soil was constructed to analyze the effective working range and temperature distribution characteristics of the microwave-irradiated soil. Second, using the 2.45 GHz microwave treatment, the following conditions were tested: soil moisture conditions of 10%, 15%, 20% and 23% (within the natural moisture content range). The loess and black soil were treated by microwave irradiation for 1–12 min, respectively (1 min/time increment). A single-factor experiment was designed to explore the influence of these factors on the soil heating law. The results show that the two soil surface temperatures are positively correlated with the soil moisture content, both of which satisfy $T_{\text{surface}23\%} > T_{\text{surface}20\%} > T_{\text{surface}15\%} > T_{\text{surface}10\%}$, and the surface temperature of black soil is higher than that of loess. According to the experimental results of the internal temperature distribution of loess and black soil irradiated by microwaves, the surface equations of “irradiation time–soil depth–soil temperature” and “irradiation time–soil moisture content–soil temperature” were constructed by surface fitting. When the irradiation time and moisture conditions are the same, the average temperature inside the irradiation area satisfies $\bar{T}_{\alpha \text{ black soil}} > \bar{T}_{\alpha \text{ loess}}$. The results of long-term microwave soil heating preliminarily confirmed the feasibility of microwave soil disinfection and the optimal conditions of microwave irradiation in loess of North China and Northeast black soil, which provides a certain reference for the study of soil-borne diseases inactivation at high temperature.

Keywords: long-term microwave; soil disinfection; temperature field; soil type; heating law



Citation: Sun, X.; Zhao, C.; Yang, S.; Ma, H.; Zhai, C. Simulations and Experiments of Soil Temperature Distribution after 2.45 GHz Long-Term Microwave Treatment. *Agriculture* **2022**, *12*, 909. <https://doi.org/10.3390/agriculture12070909>

Received: 2 June 2022

Accepted: 21 June 2022

Published: 23 June 2022

Publisher's Note: MDPI stays neutral with regard to jurisdictional claims in published maps and institutional affiliations.



Copyright: © 2022 by the authors. Licensee MDPI, Basel, Switzerland. This article is an open access article distributed under the terms and conditions of the Creative Commons Attribution (CC BY) license (<https://creativecommons.org/licenses/by/4.0/>).

1. Introduction

With the popularization of large-scale industrial agriculture, soil-borne diseases and stubborn weeds have become important factors for soil ecological imbalance, causing a decline in cultivated soil quality, thus affecting crop quality and crop yield reduction [1–3]. There are a variety of soil-borne diseases, and they can have concealed, rapid, wide-spread and serious effects on crop quality. It is difficult to accurately monitor such diseases and to provide early warning and precise prevention and control. To prevent the adverse effects of

soil-borne diseases and stubborn weeds on crops, it is necessary to disinfect the soil before cultivation [4].

Soil disinfection is mainly divided into two methods: chemical and physical. The chemical method is represented by fumigation technology, which is mainly used to kill insects, sterilize, and prevent weeds by applying pesticides to the soil [5]. Physical methods are mainly used to prevent and control diseases, insects, and grasses by increasing the internal temperature of the soil, which is mainly achieved through the use of solar energy and steam soil disinfection [6]. Physical methods for the prevention and control of crop diseases and insect pests are generally considered green, but insufficient internal soil temperature has always been the main reason that most physical soil disinfection methods cannot achieve ideal control [7]. Therefore, microwave technology, which enables soil to be rapidly heated both internally and externally, has more prominent advantages and wider application prospects in soil disinfection [8].

As a new soil disinfection method, microwaves were proposed in the 1980s. Since microwaves cause polar molecules in the medium to oscillate strongly, microwave soil disinfection has a macroscopic effect of penetration similar to soil fumigation [9]. In one study of soil heating using a microwave oven as a microwave-generating device, it was found that the highest soil temperature was between 2 and 5 cm below the surface of the soil along the centerline of the waveguide [10]. Microwaves can destroy the reproductive parts of weed plants [11]. They can also inhibit the germination of grass seeds at a depth of at least 5 or 6 cm in wet soil, provided that the soil temperature around the grass seeds reaches 65~80 °C [11]. Under the action of microwaves, all nematodes in a soil sample can be killed in 15 min at 45 °C, or several seconds at 55 °C [12,13], and 120 s can kill most of the root knot nematodes in the soil at a depth of 10 cm. For 1 kg of soil with a moisture content of 6.5~27% [14], 150 s of microwave treatment can eliminate all *Pythium*, *Fusarium* and insect populations [15]. The microwave power also affects the soil heating. After 6 min of 0.54 kW microwave irradiation combined with 18 min of heat-preservation treatment, all pathogens except *Bacillus subtilis* were killed, and the killing rate reached 94% [16]. In addition, the microwave soil disinfection process has a negative impact on the soil biological community. However, it has been shown that the original dynamic balance of the soil biological community can be basically restored within one month of microwave treatment [17]. On this basis, the contents of nitrogen and other organic matter in the soil will increase, which means that proper microwave disinfection can help improve soil fertility [18]. Microwave treatment can be combined with biochar, and the appropriate addition of biochar can contribute to the growth of bacteria, including some functional bacteria, in the soil after microwave treatment, which can improve soil microbial characteristics and increase the abundance of soil microorganisms [19,20].

There are differences in the heat capacity and thermal conductivity of different components among soils, so different soil types change the effect of microwave soil disinfection [21]. When the microwave irradiation conditions are the same, the heating rate of dry clay is faster than that of dry sand [22]. Microwave irradiation for a short period of 10~60 s can cause the maximum temperature inside the soil to reach 60 °C [23], which is the lethal temperature of some pathogenic bacteria and nematodes. However, the local high temperature generated by short-term microwaves is not enough for effective soil disinfection, and it takes several minutes or even longer to meet the needs of field weeding. To address the abovementioned problem, a combination of modeling simulation and experimental verification was used to study the long-term microwave-irradiated soil heating law [24]. Loess from North China (Beijing) and black soil from Northeast China (Jilin) were selected as the test materials. Using a 2.45 GHz microwave generation test bench, the law of long-term microwave irradiation soil was analyzed by changing the soil moisture content and microwave irradiation time. The long-term microwave soil heating law provides strong scientific guidance for the implementation of microwave soil disinfection under different soil conditions.

2. Materials and Methods

2.1. Simulation Model of the Soil Model Temperature Field under Microwave Action

Here, soil disinfection involves converting microwave energy into heat energy in the soil. Combined with soil heat conduction, the temperature of the soil during soil disinfection can reach lethal conditions for pathogens, insects and grass seeds. Therefore, this paper mainly studies the heating law of long-term microwave irradiation on soil. The thermal energy in the soil is mainly generated by the vibration of polar molecules, which is mainly due to the water in the soil. At the microwave frequency of 2.45 GHz, the electric field and the magnetic field continuously switch phases at a speed of 2.45 billion times per second, and the field energy of the alternating electric field is converted into heat energy in the soil [25]. Since the positive and negative charge centers of the water molecules do not overlap, and one end is positively charged and the other end is negatively charged, the water molecules in the soil change with the electromagnetic field during the swinging process. The water molecules oscillate back and forth rapidly under the action of microwaves, resulting in friction. The hydrogen bonds between water molecules are disrupted, and the intermolecular forces accelerate the conversion of microwave energy into heat energy, which causes the soil temperature to rise rapidly.

The speed of microwaves in vacuum is equivalent to the speed of light, and the frequency conversion is extremely fast, which is an inherent characteristic and also the reason the medium is heated inside and outside at the same time under the action of microwaves. The unique penetrability exhibited by microwave soil disinfection makes the internal temperature of the soil rise rapidly, but this penetration is not infinite. In the process of microwave soil disinfection, some of the energy will be dissipated by flowing into the lossy medium [26]. The diffusion coefficient for simultaneous heat and moisture transport γ (m^2s^{-1}) is usually defined as:

$$\gamma = \alpha + j\beta = j\omega\sqrt{\mu_0\mu \cdot \epsilon_0\epsilon} \quad (1)$$

The permeability of nonmagnetic material $\mu = \mu_0$ and the permeability of soil in microwave irradiation $\mu = 1$; combined with the penetration of microwaves in soil, the diffusion coefficient for simultaneous heat and moisture transport γ can also be expressed as:

$$\gamma = j\frac{2\pi}{\lambda_0}\sqrt{\epsilon_0\epsilon} \quad (2)$$

In the formula, α is the microwave attenuation factor (m^{-1}), $j = \sqrt{-1}$, β —phase constant, and ω —angular frequency, where frequency $\omega = 2\pi f$ in Hz, f is the period, and $f = c/\lambda_0$. λ_0 —wavelength in free space (m), c —speed of light in a vacuum (m/s), ϵ —complex permittivity, and ϵ_0 —ratio of the complex permittivity to the permittivity of free space, with a value of 8.854×10^{-12} F/m.

During microwave irradiation, the electric and magnetic fields propagate in the soil in the form of perpendicular waves [27]. The single-dimensional waveform of microwaves resembles a cosine curve, with peaks and troughs representing the maximum value in the wave energy. After microwaves enter the lossy medium soil, the electric field intensity of the first wave peak is the largest, so the maximum temperature inside the soil under the action of microwaves often occurs at a depth of several centimeters below the soil surface [28]. Microwave soil disinfection is mainly aimed at pathogenic bacteria, insects and grass seeds in the soil, most of which are condensed matter and complex compounds of proteins, fats and inorganic substances; the water content in biological cells reaches 80% [29]. Under this action, the soil becomes more vulnerable, which provides favorable conditions for microwave soil disinfection [30].

Combined with the above microwave characteristics, we can more accurately explore the heating law of long-term microwave irradiation on water-bearing soil in the cultivated layer. In this paper, COMSOL Multiphysics software is used to couple the electromagnetic field and heat transfer field and simulate the solution of the microwave soil irradiation pro-

cess [31]. First, a 3D geometric model of microwave-heated soil is established according to the experimental plan, and then the model materials, boundary conditions, and microwave-generation parameters are set, as shown in Figures 1 and 2. During the simulation process, when meshing the model, “System automatic division” is selected. For noncritical parts, a few mesh elements with poor quality (less than 0.01) will not affect the convergence of the entire model. In the simulation solution settings, “Full Coupling” is selected in the “Steady State Solver” to solve linearly. Finally, the established microwave soil irradiation electromagnetic field was added to the “object and fluid heat transfer (ht)” physical field for coupling. To explore the soil temperature distribution law at different irradiation times, “transient simulation” was selected in the coupling simulation. Table 1 shows the main physical parameters that need to be manually set in the microwave irradiation simulation and the real and imaginary parts of the dielectric loss of different water-bearing soils at 2.45 GHz frequency [32].

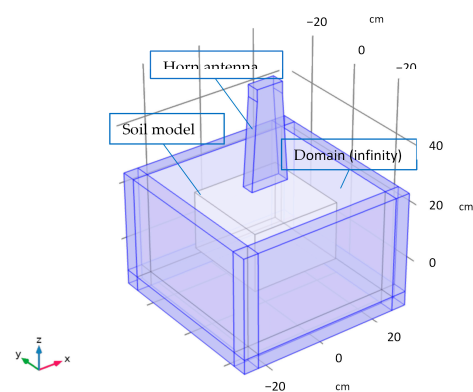


Figure 1. Construction of the microwave simulation model.

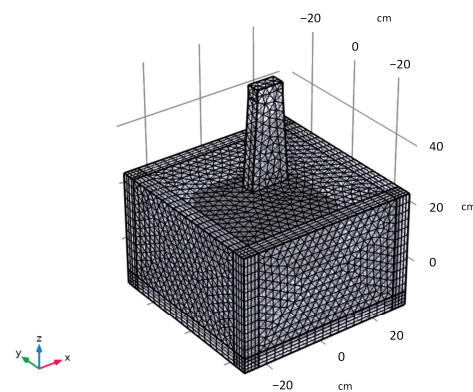


Figure 2. Meshing of the microwave irradiation simulation model.

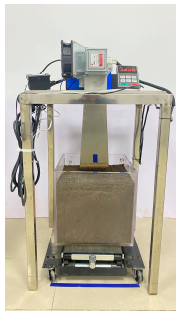
2.2. Microwave Soil Irradiation Test Bench

The microwave soil irradiation test bench is mainly composed of three parts. The first is the microwave generator and its control device, which mainly includes a magnetron, a horn-shaped waveguide, a microwave frequency conversion power supply, a microwave controller, a power display meter, and a fixture; the second part is the object of microwave action, mainly including soil, an acrylic box and a movable lifting platform; and the third part is the soil temperature acquisition device, mainly including the soil surface temperature acquisition device infrared thermal imager. A sensor matrix composed of 30 PT100 temperature sensors is used to acquire temperature values at different depths in the soil and match 5 signal acquisition modules. The main equipment and materials of the microwave soil irradiation test are shown in Table 2.

Table 1. Main parameter settings of microwave soil irradiation temperature field simulation.

Simulation Parameters	Value (Unit)	Simulation Parameters	Value (Unit)
Soil domain length (L1)	30 [cm]	Conductivity	0 (S/m)
Soil domain width (L2)	30 [cm]	Dielectric loss factor (ϵ'')	0
Soil domain height (H)	20 [cm]	Air relative permittivity	1
Waveguide to soil distance (gap)	5 [cm]	Meshing maximum element size	C_const/frequency/4
Incident frequency (frequency)	2.45 [GHz]	Meshing minimum element size	0.1
Transmit power (power)	2000 [W]	Meshing maximum element growth rate	1.5
pml thickness (t_pml)	5 [cm]	Curvature factor	0.6
Relative permeability (μ_r)	1	Narrow area resolution	0.5
Soil thermal conductivity (k_iso)	0.6 [m·k]	Soil moisture content (M)	0.11
Soil constant pressure heat capacity (Cp)	900 [J/(kg·k)]	Density (ρ)	1220 [kg/m ³]
The mass fraction of water in the soil	Re (eps)	The mass fraction of water in the soil	Im (eps)
0.021	2.99297	0.021	0
0.168	6.23886	0.168	0.76203
0.19	9.63988	0.19	1.10192
0.248	17.146	0.248	1.89194
0.292	23.63777	0.292	3.62815
0.335	26.90753	0.335	5.08877

Table 2. Main equipment and materials of the microwave soil irradiation test bench.

Equipment (Material)	Specification (Model)	Quantity	Manufacturer	Microwave Soil Irradiation Test Bench
Magnetron	2 M 362	1	LG, Seoul, Korea	
Waveguide	30 × 12.5 × 4.5 cm	1	MEGMEET Electric Co., Ltd., Shenzhen, China	
Microwave frequency conversion power supply	WepeX-1000B	1	MEGMEET Electric Co., Ltd., Shenzhen, China	
Microwave controller	WepeX-C1	1	MEGMEET Electric Co., Ltd., Shenzhen, China	
Power display meter	D69-2049	1	Elecall Electric Co., Ltd., Shenzhen, China	
Fixture	100 × 60 × 60 cm	1	Self-made	
Acrylic box	30 × 30 × 30 cm	1	Hualian Acrylic Factory, Xiamen, Fujian, China,	
Soil	2.25 × 10 ⁻² m ³	-	Self-collection	
Movable lift platform	46 × 32 × 20 cm	1	Karlon Hardware Store, Jiaxing, Zhejiang, China	
Infrared thermal imager	Testo 865	1	Testo AG, Germany	
Temperature sensor	PT100	30	Senxtee Electric Co., Ltd., Hangzhou, China	
Signal acquisition module	DS18B20	4	Senxtee Electric Co., Ltd., Hangzhou, China	

2.3. Microwave Soil Irradiation Test Method

Common microwave soil disinfection facilities often operate such that microwaves enter the soil directly through the waveguide [33]. If a cavity with a metal reflective wall is selected for the test, the effect of microwave action will be increased, but it will also cause deviations in the results due to the inconsistency with the actual form of microwave soil disinfection [34]. In this paper, the microwave frequency of 2.45 GHz (or similar values for countries with different legislation) is used for soil irradiation experiments. Too low a frequency will hinder the energy absorption of the soil medium, while too high a frequency is not suitable for mobile soil disinfection equipment. In the test, the microwave magnetron is connected to the horn-shaped waveguide, the waveguide port is perpendicular to the irradiated soil, the acrylic box containing the soil is placed directly under the waveguide port, and the two centerlines of the waveguide port and the centerline of the acrylic box are measured by moving the lift table; they are all on the same plane. Considering the uneven soil and the heat dissipation problem of the waveguide, the lifting platform is adjusted to make the distance between the waveguide port and the soil surface 5 cm [35]. It is worth noting that the value displayed on the microwave controller panel is the power after microwave conversion, which is approximately 0.6 times the actual power [36]. Therefore, the microwave controller needs to be adjusted before the test to control the actual output power. When the value of the microwave controller is adjusted to a numerical value of 1280, the actual microwave output power displayed by the power display meter panel can be stabilized at 2000 W.

The loess used in the experiment was taken from the National Experimentation for Precision Agriculture (40°10'31" N, 116°26'10" E, Beijing, China). The soil type is silty loam with a uniform soil distribution [37]. The black soil was taken from the teaching and research base of Jilin Agricultural University (125°24'44.136" N, 43°49'23.2104" E, Changchun City, Jilin Province, China). It is a typical black soil with high humus content [38]. Compared with the loess in North China, the proportion of clay content is relatively low, and the cohesive strength is not as good as that of loess. Humus has strong chemical activity and colloidal properties, and often undergoes a series of changes with clay minerals to form mineral and organic colloid complexes. These colloids have strong adsorption properties for metal elements or form chelates with ionic metal elements to fix them in the soil. The content of some elements in the soil often has a certain positive correlation with the content of organic matter in the soil, so the content of the elements measured in black soil is often higher than that in other soils [39]. The saturated water content of both soils is approximately 23% [40,41]. When preparing soils with different water contents in the experiment, first, the collected soils were passed through a 2 mm sieve [42], put into a dryer, and dried at 105 °C for 24 h [43]. Then, according to the calculation method of soil moisture content, the soil was injected into distilled water and stirred until uniform and set aside for 24 h. Since the main purpose of the experiment in this paper was to explore the heating law of the loess and black soil under long-term microwave radiation, the physical and chemical properties of soil samples before and after microwave treatment were not detected and analyzed.

In the experiment, the North China loess and Northeast black soil were irradiated with microwaves for a period of 1–12 min (1 min increments). The purpose was to explore the microwave heating law on the soil surface and in the plow layer (the top 1–20 cm), where crop diseases and insect pests are prone to occur [44]. For the experiment, four soil moisture content nodes were selected within the range of extreme conditions, which were 10%, 15%, 20%, and 23%. After the microwave frequency conversion power supply was powered on, the power meter panel value displayed 2000 W to start timing. After the irradiation was completed, the microwave frequency conversion power supply was turned off, and the lifting platform was pulled out to collect soil surface temperature data. The method was as follows: the distance between the camera of the infrared thermal imager and the soil surface was approximately 50 cm, forming an included angle of 45°, and the image was captured after the four edges of the soil surface completely entered the display of the infrared thermal imager. The images were marked by the Testo IR Soft software for the location of the maximum temperature on the soil surface and to acquire numerical values and adjust the temperature scale. The surface temperature is greatly affected by environmental factors, so this operation was generally completed within 5 s after the irradiation was stopped. Immediately after the soil surface temperature was acquired, the inner depth of the soil was acquired. The method was to place the centerline of the PT100 temperature sensor matrix and the centerline of the acrylic box on the same plane, observe the scale line on the PT100 sensor probe, and insert the sensor matrix vertically into the soil at increments of 1 cm. The temperature acquisition time for each layer was approximately 8 s with an overall rate of 20 s per layer. Due to the thermal insulation properties of the soil and the relatively ideal conditions of the laboratory, the soil temperature collection process of 1–20 cm did not have a great impact on the overall test results. The PT100 sensor transmitted the temperature information to the computer through the acquisition module and converted it into a temperature value through Smacq | M Console V0.6 software for storage. The temperature obtained in the microwave soil irradiation test is shown in Figure 3. During the test, the magnetron was covered with a metal shell to avoid microwave interference with the normal operation of other electronic components. The operator wore electromagnetic protective clothing throughout the process [45].

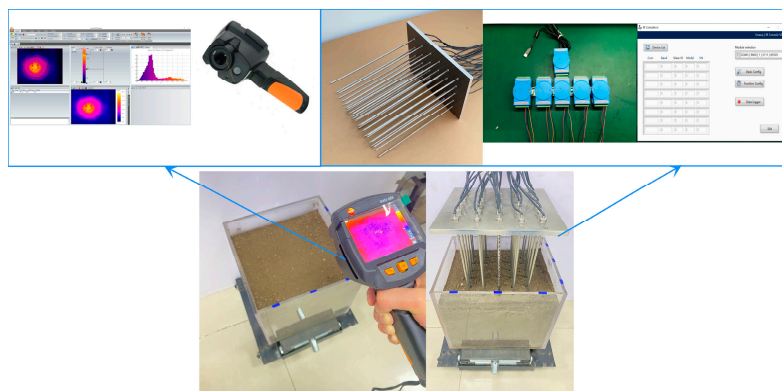


Figure 3. Soil temperature acquisition during the microwave irradiation test.

The single-factor test method was used to explore the influence of irradiation time, soil moisture content and soil depth on the soil heating law and to analyze and compare the heating law of loess and black soil. The test results not only play a guiding role in the microwave soil disinfection operation under different soil conditions, but also provide a strong scientific basis for microwave research on soil composition changes and biodiversity.

3. Results and Discussion

3.1. Simulation Results of Microwave-Irradiated Soil

Microwave soil disinfection is often aimed at diseases, insects, and weeds inside the soil. Compared with the interior of the soil, the soil surface can be fully exposed to air and ultraviolet rays, but there are still a certain number of pathogenic bacteria, grass seeds and other crop hazards, so it is necessary to explore the law of soil surface temperature. During the simulation of microwave-irradiated soil surface temperature, after selecting the “results-research-surface” option in the interface, the simulation results of 1–12 min of irradiation can be obtained, and the results are shown in Figure 4. To facilitate the exploration of the soil surface temperature law, the temperature scale was uniformly adjusted to 300–450 K after combining with the soil surface temperature range. The simulation results show that the soil surface presents a circular area after microwave irradiation, which is located directly under the waveguide. With increasing irradiation time, the soil surface temperature gradually increases, the circular area increases, and the diameter approaches the long side of the waveguide port. In the simulation results of the soil temperature field, when the soil moisture content is 10%, the maximum soil surface temperature after 12 min of microwave irradiation is 448.6 K (174.5 °C), which is in the center of the circular area.

COMSOL Multiphysics was used to simulate the high-speed vibration of polar water molecules in the soil under the action of microwaves to generate heat and combine multiple soil components in the process of soil heat conduction. Figure 5 shows the simulation results of the internal heating law of the soil irradiated by microwaves for 1~12 min, showing the temperature change law of the central section (X-Z plane) of the soil model. The internal temperature of the soil increases with increasing irradiation time and gradually penetrates into the soil. However, due to the conversion and dissipation of energy in the process of microwave irradiation and soil heat conduction, it becomes increasingly difficult to heat the interior of the soil, so the high-temperature area inside the soil presents an inverted cone. The highest temperature inside the soil appears just below the waveguide. Therefore, the soil temperature at different depths along the vertical line in the model is selected for the acquisition of the simulation results of the internal soil temperature. After the simulation is completed, “3D Section” is selected in the “Result-Research” option, and the vertical line in the soil model is determined by the coordinates of (0,0,0) and (0,0,20), as shown in Figure 6. After the vertical line is divided in centimeters, the simulation software draws the soil temperature diagram at each point and defines the “Temperature Expression” as “T” in units of “K” before plotting. Figure 7 shows the temperature values of the soil model at the

mid-perpendicular position after 12 min of microwave irradiation; the initial temperature of the soil at room temperature was set to 298.2 K.

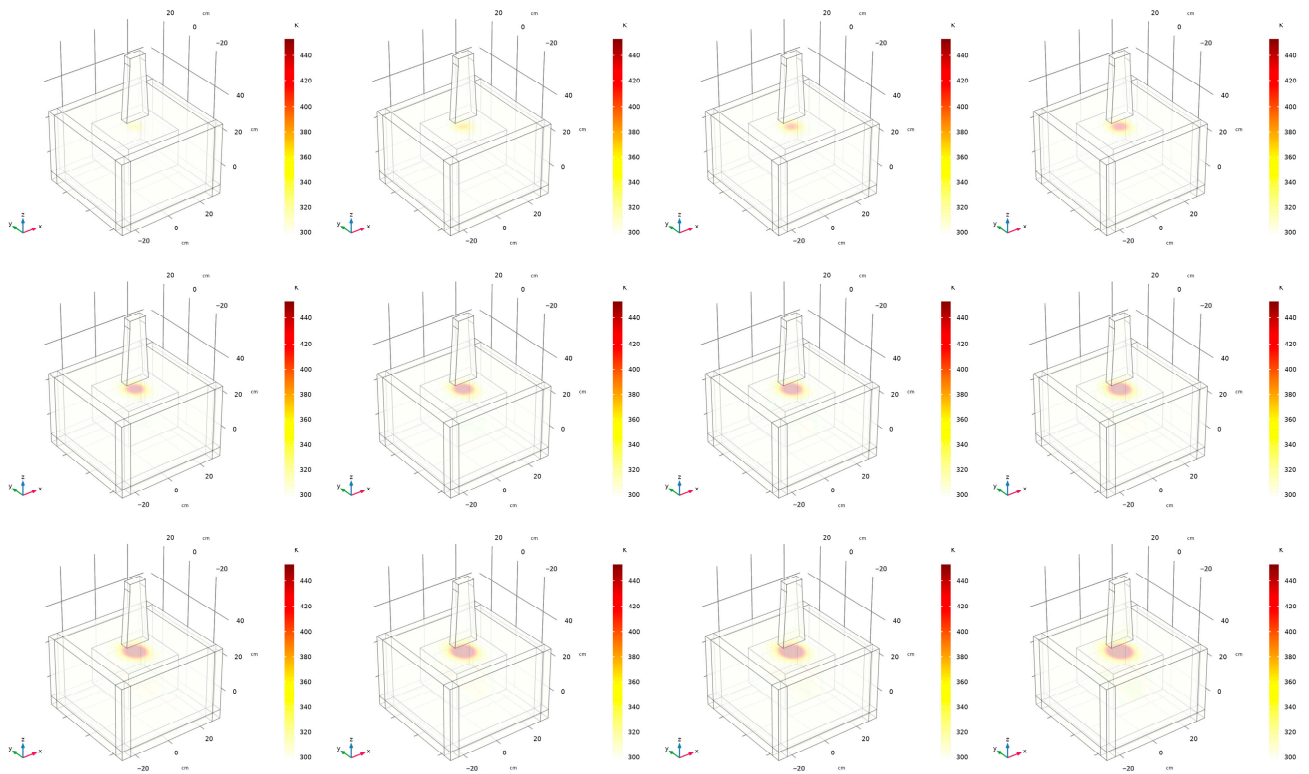


Figure 4. Surface temperature law of the microwave-irradiated soil model.

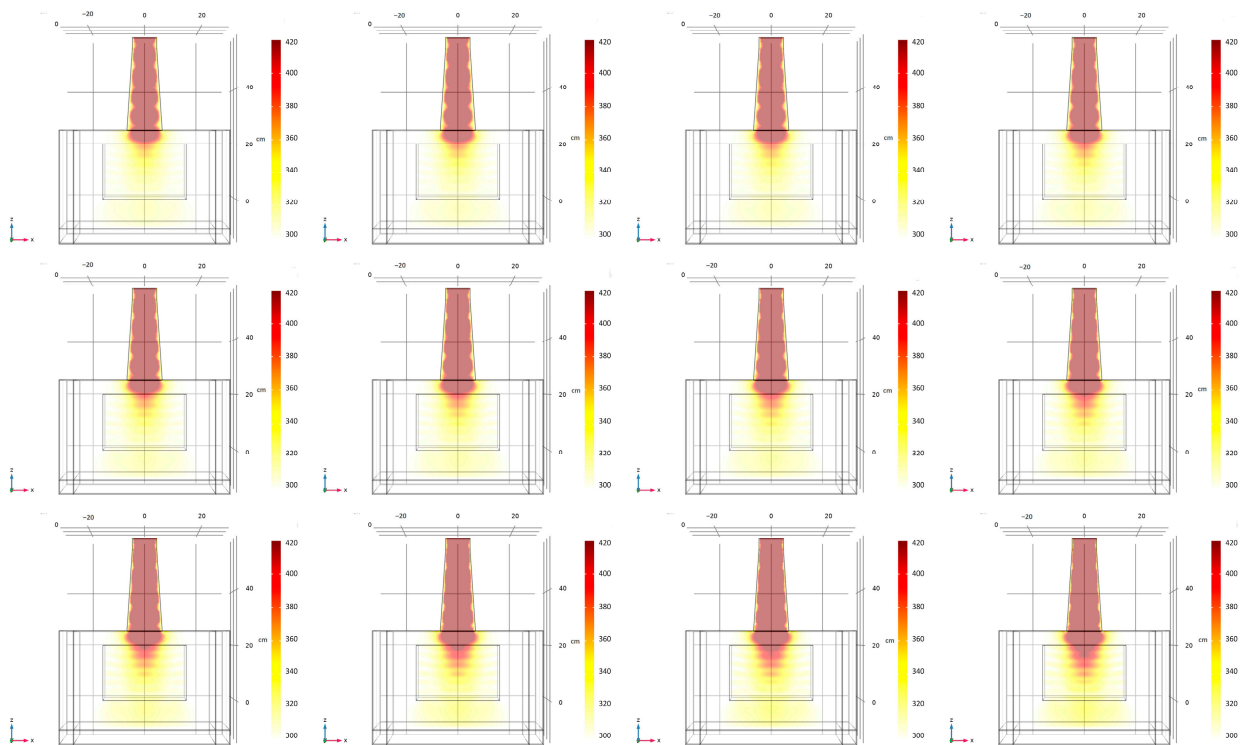


Figure 5. Temperature variation law of the microwave-irradiated soil model.

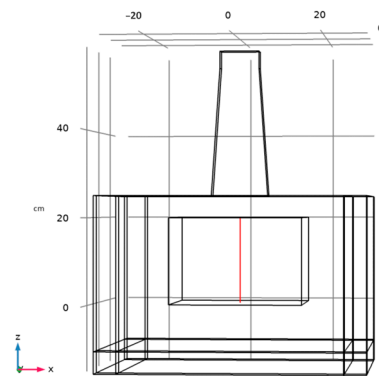


Figure 6. Acquisition of midline temperature values for the soil model.

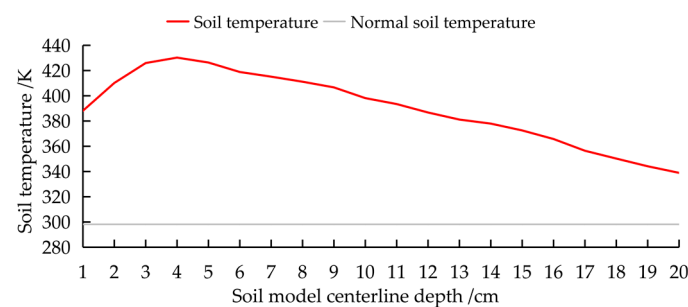


Figure 7. Soil model midline temperature plot.

The simulation results after microwave irradiation for 5 min show that the maximum temperature inside the soil is 374.2 K, which meets the lethal temperature of most pathogenic bacteria, grass seeds and resistant plant viruses. Preliminarily, this shows the feasibility of long-term microwave irradiation in soil disinfection operations, but the simulation is carried out under ideal conditions by default. The soil has ideal characteristics, such as uniform texture and the same porosity. Therefore, there must be some gaps between the test results and the simulation results under the same irradiation conditions, and it is necessary to further explore the soil heating law in combination with the long-term microwave soil irradiation test.

3.2. Results of Microwave-Irradiated Soil Surface Test

After microwave irradiation of the soil, due to the evaporation of water in the soil within the irradiation range, a circular area of low water content soil appears on the soil surface, which is lighter in color than the surrounding soil. The size of the area changes with the irradiation time and is located directly under the waveguide. Figure 8 shows the soil surface image of 20% water-bearing loess and black soil after 12 min of microwave irradiation. After actual measurement, it is found that the maximum diameter of the two dry soil areas can reach approximately 135 mm after 12 min of irradiation, which is similar to the length of a rectangular waveguide. This is almost consistent with the simulation results of the soil surface temperature. In the 12 min simulation results, the diameter of the high-temperature region directly under the waveguide is also similar to the length of the long side of the waveguide. Figures 9 and 10 show the variation law of the diameter of the circular area on the soil surface after the microwave exposure of loess and black soil, respectively. When the microwave irradiation time is the same, the relationship between the diameter (R) of the circular area irradiated on the two soil surfaces and the soil moisture content is $R_{\text{surface23\%}} > R_{\text{surface20\%}} > R_{\text{surface15\%}} > R_{\text{surface10\%}}$. Under the conditions of 10%, 15%, 20%, and 23% soil moisture, the diameter of the circular area after 12 min of microwave irradiation is close to the length of the long side of the waveguide.



Figure 8. Soil surface of loess (left) and black soil (right) irradiated by microwaves for 12 min.

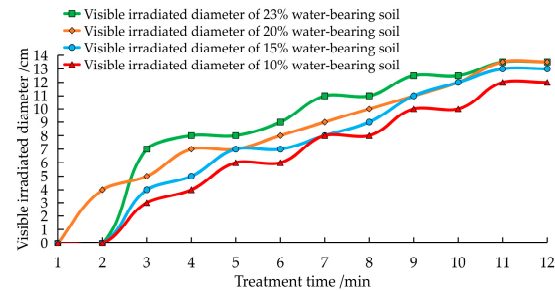


Figure 9. Diameter of circular area on the surface of loess irradiated by microwaves.

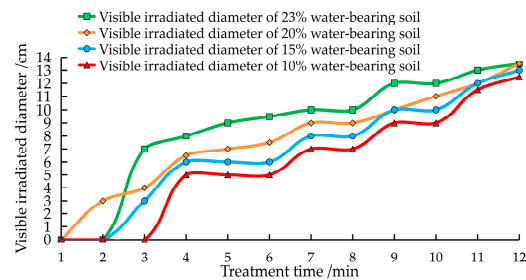


Figure 10. Diameter of circular area on the surface of black soil irradiated by microwaves.

Figures 11 and 12 show the thermograms of the surface temperature of loess and black soils with moisture contents of 10%, 15%, 20%, and 23% after long-term microwave irradiation. After the soil surface is irradiated, the thermal map shows a circular area similar to the simulation results, and the highest temperature value is mostly located in the center of the elliptical area. The temperature scale range is adjusted to 25–180 °C. The microwave soil surface irradiation results show that the soil surface temperature was positively correlated with the microwave irradiation time and soil moisture content. Comparing Figures 11 and 12, it is found that the diameter and brightness of the bright yellow area on the surface of black soil are generally higher than those of loess, which indicates that under the same irradiation conditions, black soil has a higher surface temperature value.

The broken line graphs of the surface temperature of loess and black soil are shown in Figures 13 and 14. When the microwave irradiation time is 1 or 2 min, the soil surface temperature fluctuates due to the influence of environmental factors. After 2 min, the soil surface temperature increased steadily with increasing irradiation time, and the rising rate tended to be flat after 8 min. In the process of irradiating loess and black soil surfaces by microwaves, the soil surface with more water molecules can generate more heat. Therefore, under the same microwave irradiation time, the relationship between the surface temperatures of the two soils is $T_{\text{surface}23\%} > T_{\text{surface}20\%} > T_{\text{surface}15\%} > T_{\text{surface}10\%}$. Figure 15 shows the comparison of the surface temperature of loess and black soil under the same microwave irradiation conditions. Except for individual test points affected by environmental factors, the surface temperature of black soil is higher than that of loess, namely, $T_{\text{black soil}} > T_{\text{loess}}$.

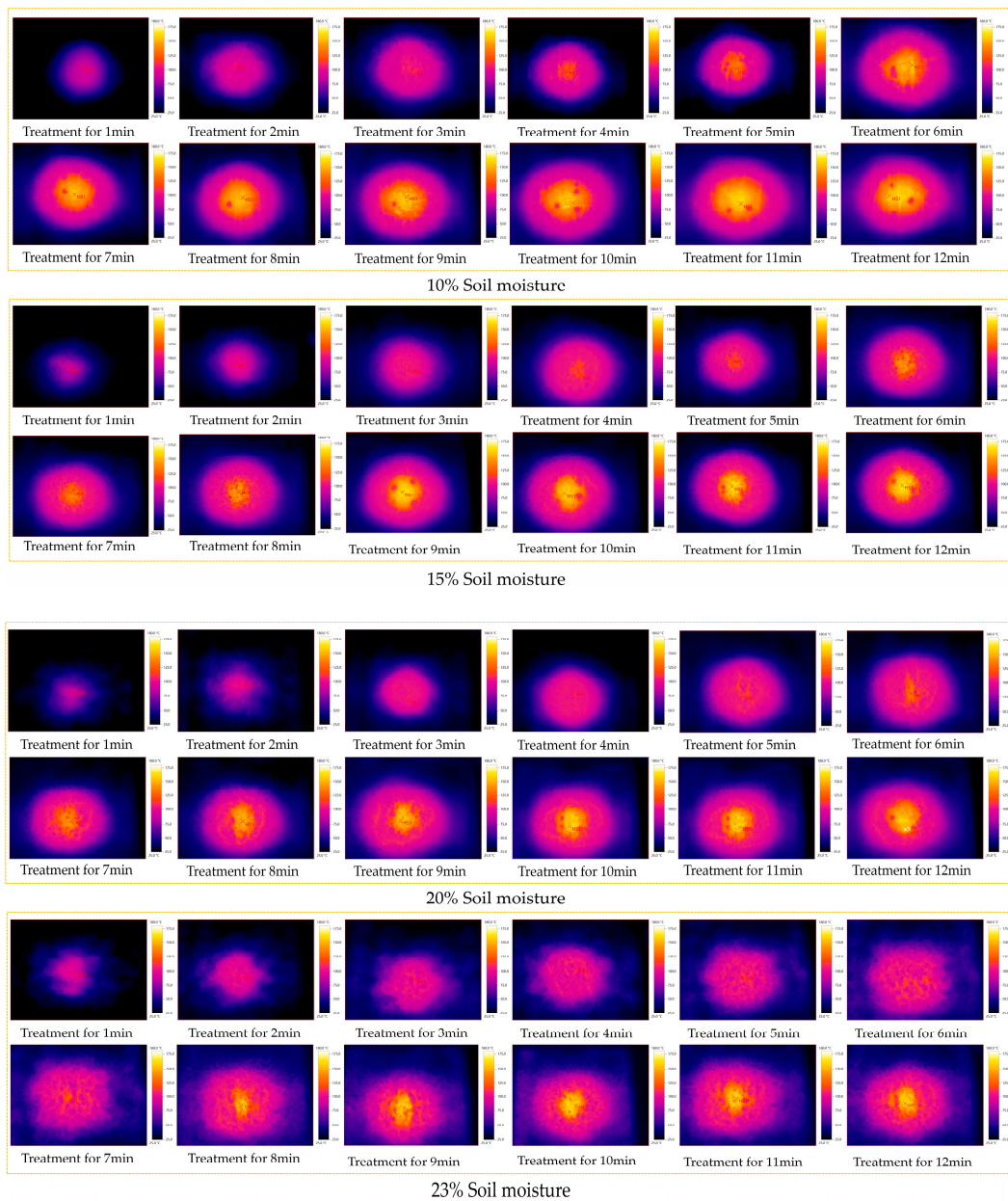


Figure 11. Thermal image of loess surface irradiated by microwaves.

The surface temperature difference between North China loess and Northeast black soil after microwave irradiation is mainly caused by the different composition ratios of solid, liquid, and gas three-phase materials between the soils. The soil volumetric heat capacity C_v can be expressed by Equation (3):

$$C_v = mC_v \cdot V_m + oC_v \cdot V_o + \omega C_v \cdot V_w + \alpha C_v \cdot V_a \quad (3)$$

where mC_v , oC_v , ωC_v and αC_v represent the volumetric heat capacities of soil minerals, organic matter, water, and air, respectively. V_m , V_o , V_w , and V_a are the volume ratios of soil minerals, organic matter, water and air per unit volume of soil, respectively.

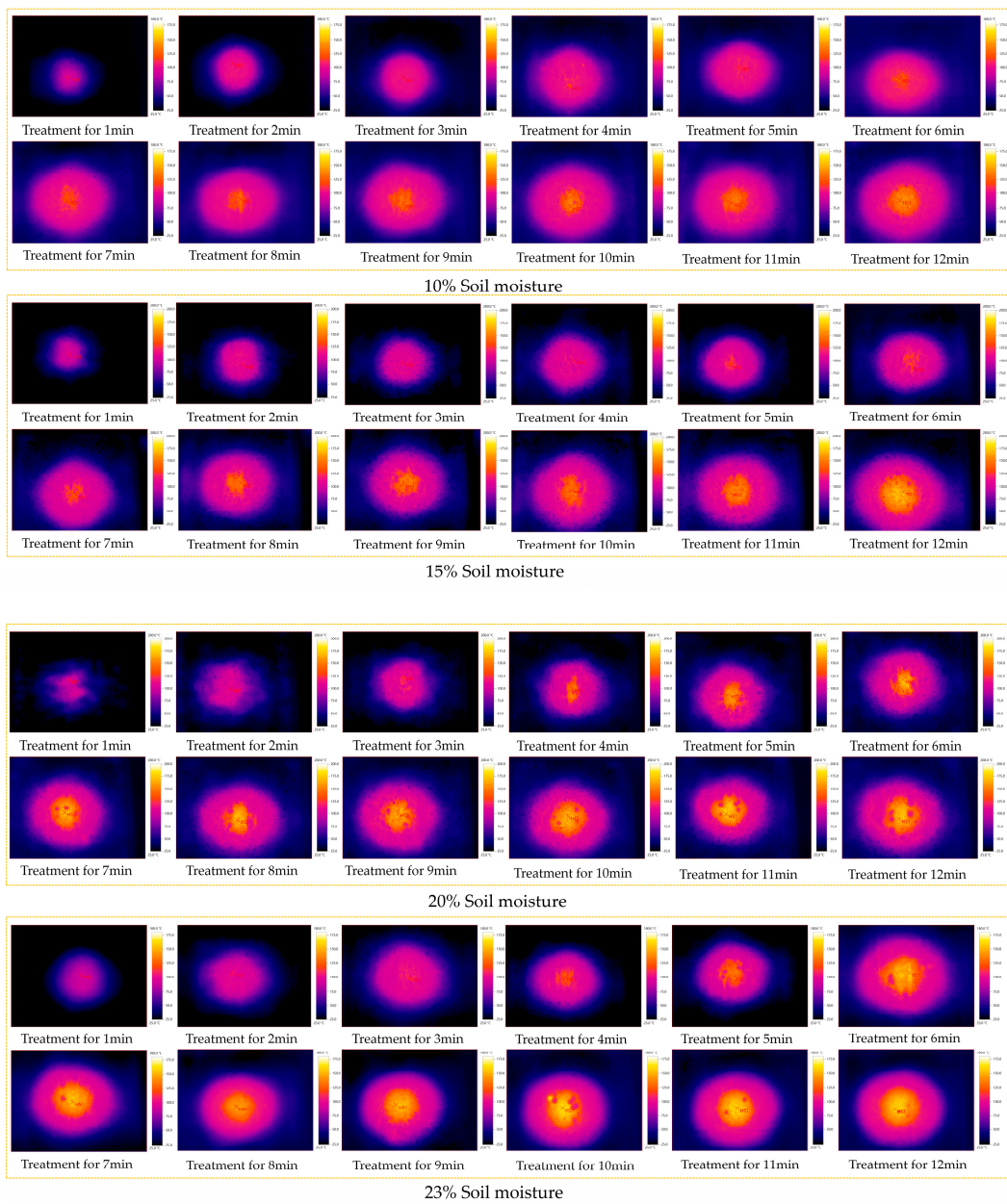


Figure 12. Thermal image of the surface of water-bearing black soil irradiated by microwaves.

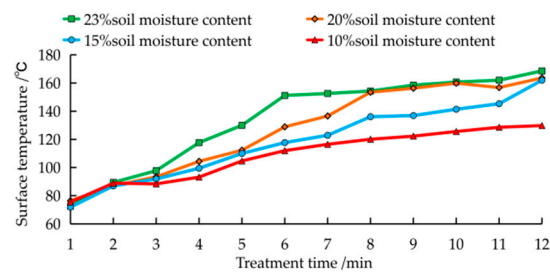


Figure 13. Surface temperature of loess irradiated by microwaves.

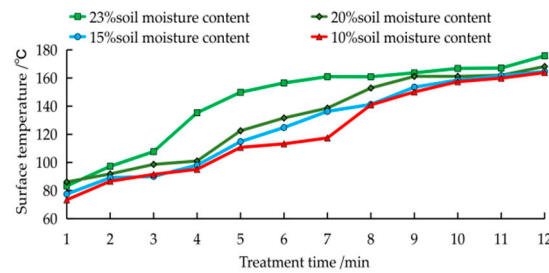


Figure 14. Surface temperature of black soil irradiated by microwaves.

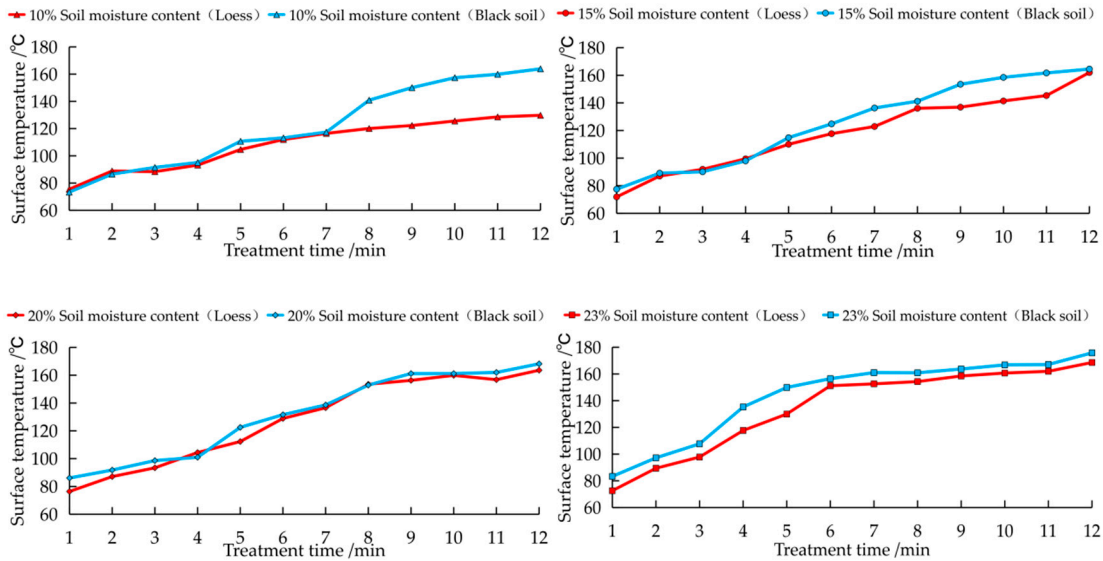


Figure 15. Comparison of surface temperature between loess and black soil.

Since the value of the air heat capacity V_α is negligible, the soil heat capacity can be simplified to Equation (4):

$$C_v = 1.9V_m + 2.5V_0 + 4.2V_w \tag{4}$$

The heat capacity of water is the largest, and that of gas is the smallest in the three-phase material composition of soil solid, liquid and gas; minerals and organic matter are located between the two. During microwave irradiation, both soils were placed in an acrylic box with a side length of 30 cm, and the water-containing soil in the acrylic box was replaced according to the test requirements. Therefore, when the soil moisture content is the same, the soil solid-phase composition is the main factor affecting the microwave soil heating law.

The content of humus is higher in the black soil of Northeast China, and the content of quartz is higher in the loess of North China. The volumetric heat capacity C_v of quartz in the soil component is $2.163 \text{ (J}\cdot\text{g}^{-1}\cdot\text{°C}^{-1}\text{)}$, and the volumetric heat capacity C_v of humus is $2.525 \text{ (J}\cdot\text{g}^{-1}\cdot\text{°C}^{-1}\text{)}$. The heat capacity of humus in soil is larger than that of minerals, and the difference in mineral heat capacity is small. Therefore, the size of the soil heat capacity C_v mainly depends on the humus content in the soil. In addition, the thermal conductivity K is also an important factor affecting the soil temperature, which refers to the value of the temperature rise or fall after the unit volume of soil flows into or out of λ heat. The unit is $\text{m}^2\cdot\text{s}^{-1}$, which is expressed by Equation (5) as:

$$K = \frac{\lambda}{C_v} \tag{5}$$

When the soil moisture content is the same, the thermal conductivity of humus in the soil component (1.225×10^{-2}) is smaller than that of quartz (4.427×10^{-2}). Under the same microwave irradiation conditions, if the loess and black soil receive the same energy, due to the relatively large thermal conductivity K of the loess, the soil temperature changes rapidly, and the temperature dissipates quickly, while the black soil has a small thermal conductivity and the soil temperature changes slower, so the black soil has a higher surface temperature in the test results. In the exploration of the surface temperature law of the 1–12 min microwave irradiation test, the maximum temperature after the irradiation of loess was $168.6\text{ }^{\circ}\text{C}$, and the maximum temperature after the irradiation of black soil was $175.8\text{ }^{\circ}\text{C}$, both obtained when the maximum irradiation time was 12 min and the maximum soil moisture content was 23%.

3.3. Test Results of the Internal Temperature of the Soil Irradiated by Microwaves

In the process of microwave soil disinfection, the internal temperature of the soil is an important factor for diseases, insects and weeds to reach the corresponding lethal conditions. In the microwave soil irradiation test, the soil temperature value in the cultivated layer was obtained through a matrix composed of 30 PT100 temperature sensors, and the temperature values of 30 points at the same depth of the soil were measured each time. Figures 16–23 show the variation law of soil temperature at 10%, 15%, 20%, and 23% water-bearing loess and black soil at 1–20 cm depth. The abscissa in the heatmap represents the test points of the 30 temperature sensors on the plane, and the ordinate represents the different depths of the soil model. To explore the law between microwave irradiation time, soil temperature and depth, the temperature scale interval in the heatmap was uniformly adjusted to $20\text{--}150\text{ }^{\circ}\text{C}$ according to the actual measured soil internal temperature. After obtaining the temperature of the 1–20 cm soil depth, it is found that the unique penetration of microwaves causes the highest temperature inside the soil to often appear several centimeters below the soil surface. When the soil moisture content is constant, the longitudinal heating of the soil under the waveguide increases significantly with increasing time during the microwave irradiation process of 1–5 min, which may be mainly attributed to the penetration of microwaves; after 5 min, the soil was irradiated with microwaves, and it was found that the increase in the internal temperature of the soil was not only deeper in the soil but also the lateral soil temperature diffusion was relatively obvious. At this point in the microwave irradiation process, the thermal conductivity of the soil plays a crucial role in the increase in the internal soil temperature.

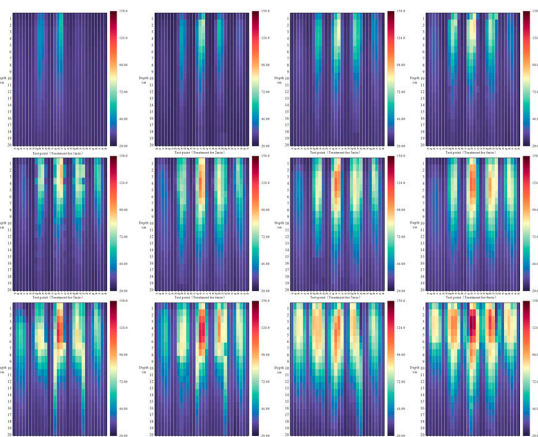


Figure 16. Heatmap of the internal temperature of 10% loess under microwave irradiation.

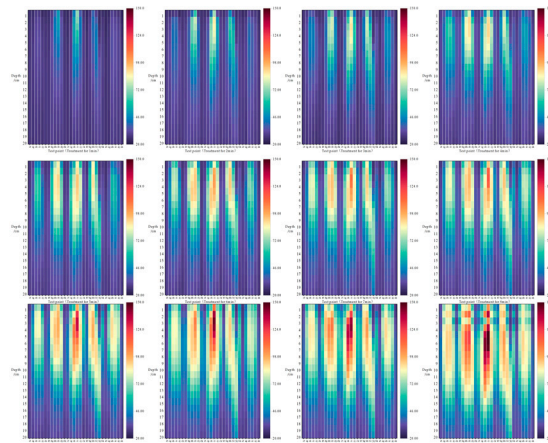


Figure 17. Heatmap of the internal temperature of 10% black soil under microwave irradiation.

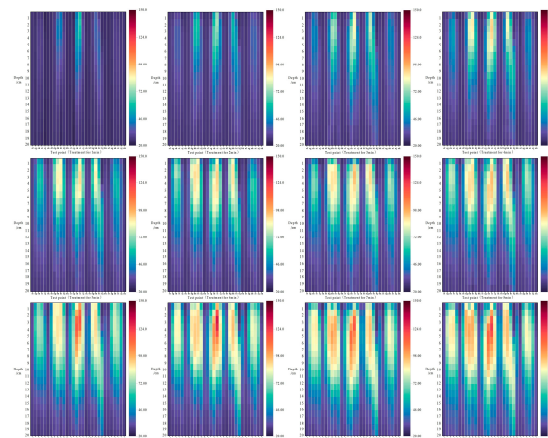


Figure 18. Heatmap of the internal temperature of 15% loess under microwave irradiation.

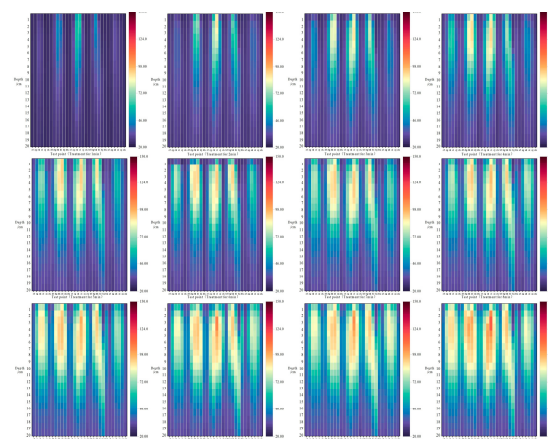


Figure 19. Heatmap of the internal temperature of 15% black soil under microwave irradiation.

The internal temperature of loess and black soil irradiated by microwaves for 1~12 min increased with increasing irradiation time. Observing the heatmaps of the two soils at 10%, 15%, 20%, and 23% moisture content, it was found that when the soil moisture content was 10%, the interior of the two soils reached the maximum temperature value. After 12 min of microwave irradiation, the maximum internal temperature of the two soils reached 141 °C (loess) and 151.6 °C (black soil), which were obtained 3 cm and 4 cm away from the soil surface. When the soil moisture content was 23%, the internal temperature of the soil, as shown in the heatmap, was lower than that of the other three soil moisture

contents. With the increase in microwave irradiation time, part of the “stripe” area did not change significantly after long-term microwave irradiation. The main reason for this phenomenon is that these test points are often distributed far away from the waveguide; after all, the scope of action of a single microwave emission unit is limited. Combined with the 1~12 min microwave irradiation of the soil surface irradiation area and the temperature change inside the soil, the rectangular area consisting of 12 temperature sensors bg~bj, cg~cj, and dg~dj is determined as the main research object within the effective operating range of the microwave unit. Figure 24 shows the effective working area, including the irradiated area.

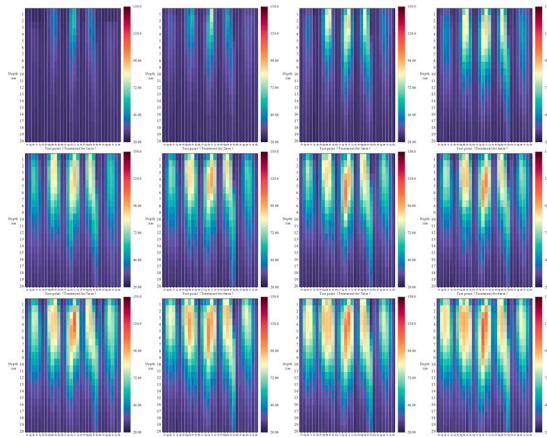


Figure 20. Heatmap of the internal temperature of 20% loess under microwave irradiation.

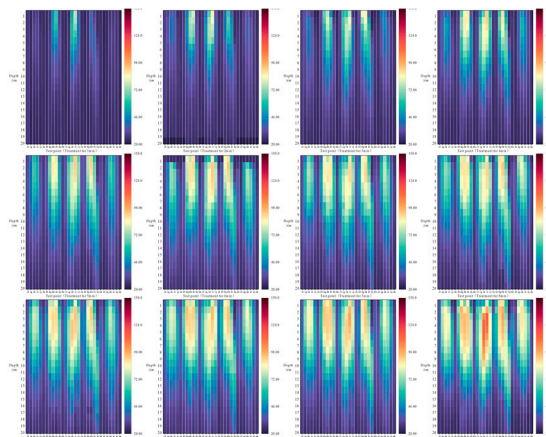


Figure 21. Heatmap of the internal temperature of 20% black soil under microwave irradiation.

In the study of the temperature law of microwave-irradiated soil, studying only the highest temperature obtained by the sensor would not be comprehensive. Combined with the simulation results and the change in soil internal temperature in each irradiation time period, a rectangular area of 160×120 mm composed of 12 temperature sensors was studied as the effective operating range of the microwave unit. Figure 25 is a schematic diagram of the soil model irradiated by microwaves. First, the soil at a depth of 20 cm in the area is divided into 20 layers, each with a height of 1 cm. Then, 12 sensors are used to obtain the soil temperature inside the effective irradiation area during the microwave irradiation period of 1~12 min. Finally, the temperature values of the soil temperature test points of each layer are averaged to obtain the average layer temperature \bar{T}_n ; the calculation method is shown in Equation (6).

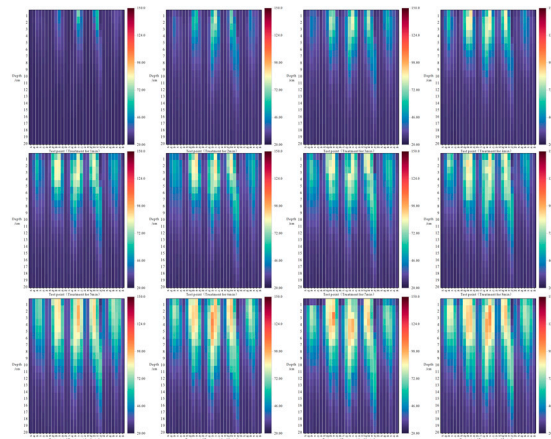


Figure 22. Heatmap of the internal temperature of 23% loess under microwave irradiation.

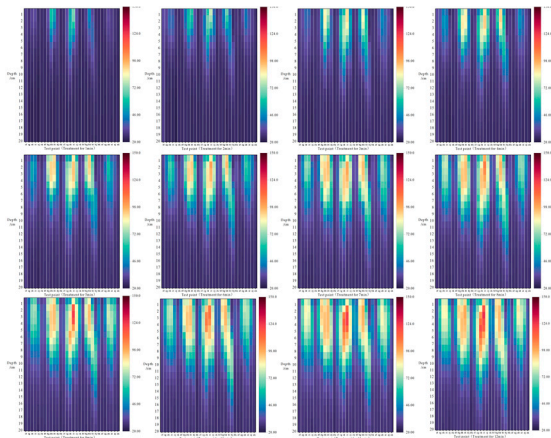


Figure 23. Heatmap of the internal temperature of 23% black soil under microwave irradiation.

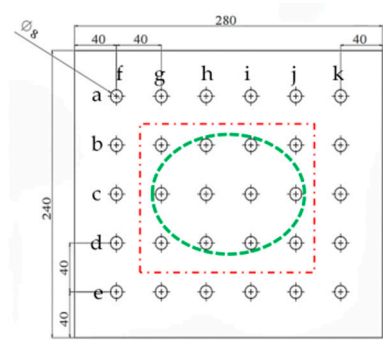


Figure 24. Effective area division of the microwave-irradiated soil surface.

$$\bar{T}_n = (T_{bg} + T_{bh} + T_{bi} + \dots + T_{dj}) / 12 (n = 1, 2, 3 \dots 20) \tag{6}$$

In the equation, \bar{T}_n is the average temperature of the soil layer, n is the soil layer number, and $T_{bg}, T_{bh}, T_{bi} \dots T_{dj}$ correspond to the temperature values obtained by the 12 sensors in the rectangular irradiation range, as shown in Figure 24. Soil depth and microwave irradiation time are used as independent variables, and the average temperature of each soil layer T_n is used as a dependent variable. The variation law of the internal temperature of loess and black soil with irradiation time and soil depth was obtained by constructing a three-dimensional surface, as shown in Figures 26 and 27. The figure intuitively reflects the internal temperature of the loess and black soils in the 1–20 cm soil

layer when the soil moisture content is 10%, 15%, 20%, and 23%. The soil temperature of loess and black soil is higher than that of other water-bearing soils when the water content is 10%, and lower than that of other water-bearing soils when the water content is 23%. When the soil moisture content is constant, the soil temperature increases with the increase in microwave irradiation time, and both soils maintain a high soil temperature in the 10~15% moisture range. The soil temperature outside this range shows a decreasing trend with the increase or decrease in soil moisture content. When the microwave soil was irradiated to 12 min, the maximum average temperature was obtained in the soil layer of 10% water-bearing loess and Northeast black soil. The maximum temperature of loess was 94 °C, which was measured in the soil layer of 3 cm. The highest temperature of black soil was 100.04 °C, which was measured in the soil layer of 4 cm.

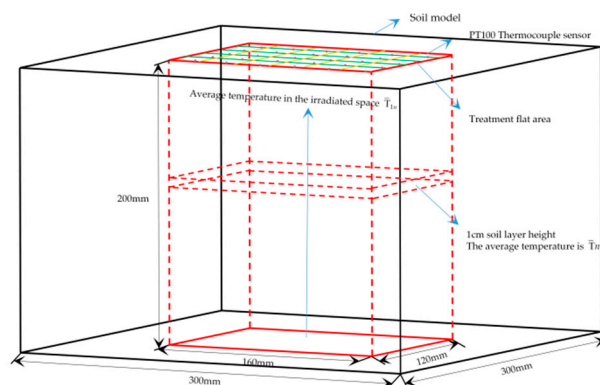


Figure 25. The division of the overall effective area of the microwave-irradiated soil model.

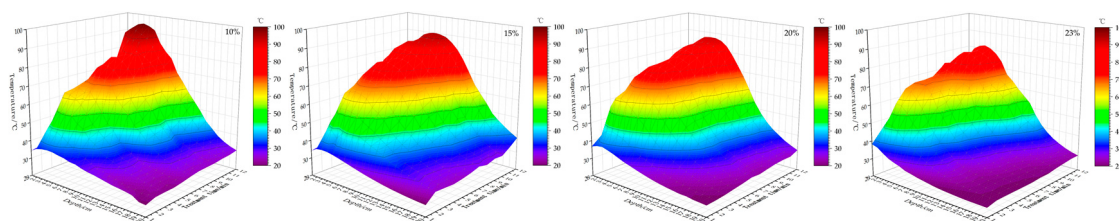


Figure 26. Variation in the internal temperature of loess with irradiation time and soil depth.

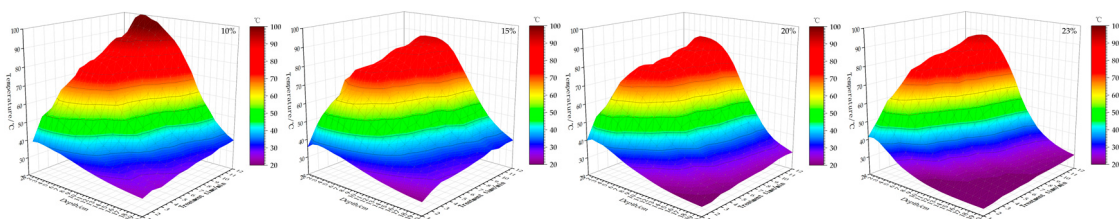


Figure 27. Variation in the internal temperature of black soil with irradiation time and soil depth.

Gaussian equation fitting was performed on the three-dimensional surface, and the temperature fitting surfaces of “irradiation time–soil depth” for loess and black soil, as shown in Figures 28 and 29, were obtained. The parameters in the surface equation and their extreme points are shown in Tables 3 and 4. It can be seen from the fitted surface that the position of the highest temperature inside the two soils approaches the soil surface with the increase in soil moisture content, from 5~6 cm in 10% soil moisture content to 1~2 cm in 23% soil moisture content. Through the surface fitting equation of the change in soil internal temperature with irradiation time and soil depth, the average temperature \bar{T}_n of any layer inside the soil of North China loess and Northeast black soil of 1~20 cm can be obtained within the microwave irradiation time of 1~12 min. Accordingly, the microwave

soil irradiation time can be used to determine whether the interior of the soil layer has reached the lethal temperature of pathogenic bacteria, insects and grass seeds in the process of microwave soil disinfection.

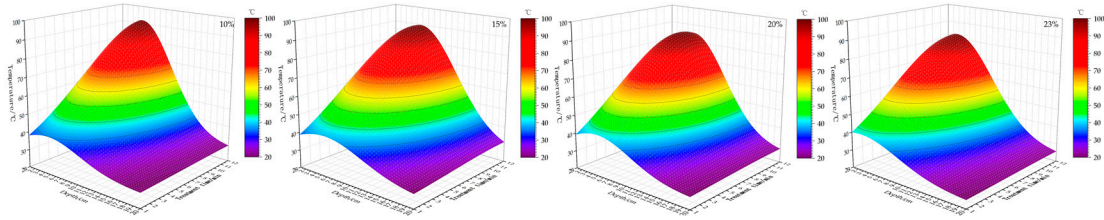


Figure 28. Fitting surface of the loess internal temperature with irradiation time and soil depth.

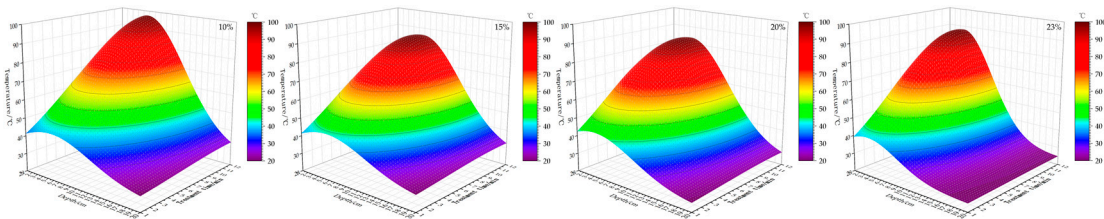


Figure 29. Fitting surface of black soil internal temperature with irradiation time and soil depth.

Table 3. Surface fitting equation of the change in the internal temperature \bar{T}_n of the soil layer with the irradiation time and soil depth (“irradiation time–soil depth” temperature fitting surface equation, the number after “±” represents the parameter range).

Equation		$\bar{T}_n = z_0 + A \exp \left\{ -\frac{1}{2} \left(\frac{x-x_c}{\omega_1} \right)^2 - \frac{1}{2} \left(\frac{y-y_c}{\omega_2} \right)^2 \right\}$						
Parameters		z_0	A	x_c	ω_1	y_c	ω_2	R^2
Soil moisture content of loess/%	10	27.77206 ± 0.58904	64.3469 ± 1.34936	4.74245 ± 0.09999	5.43662 ± 0.13654	12.54015 ± 0.40527	6.44588 ± 0.28604	0.96782
	15	26.44759 ± 1.05091	63.44349 ± 1.24698	5.58985 ± 0.11612	6.35822 ± 0.19674	11.65806 ± 0.33563	6.38847 ± 0.29611	0.9564
	20	26.0145 ± 0.80595	61.09687 ± 0.91617	4.97283 ± 0.1123	5.66393 ± 0.16698	10.56247 ± 0.23881	5.94615 ± 0.23518	0.9573
	23	24.0885 ± 0.73671	58.92115 ± 1.56181	2.66982 ± 0.26274	6.49518 ± 0.27156	12.56472 ± 0.56986	7.22563 ± 0.42097	0.95647
Soil moisture content of black soil/%	10	26.55192 ± 1.07152	70.99927 ± 1.45919	5.65879 ± 0.10169	6.58442 ± 0.17942	12.39321 ± 0.38395	6.99546 ± 0.31257	0.96756
	15	27.32122 ± 1.15636	59.66404 ± 1.12672	5.6307 ± 0.11883	6.55357 ± 0.21495	10.85128 ± 0.26614	6.36138 ± 0.2773	0.95385
	20	23.54104 ± 0.97546	61.01984 ± 1.00369	4.22685 ± 0.15539	6.68197 ± 0.22432	10.81245 ± 0.27616	6.73701 ± 0.27937	0.96293
	23	24.40695 ± 0.62829	64.38545 ± 1.04298	3.59239 ± 0.14632	5.19025 ± 0.16753	11.13109 ± 0.33009	6.19061 ± 0.28187	0.95807

The effectiveness of microwave soil disinfection is generally measured by the lethality of soil pathogens, harmful insects and grass seeds within the affected area [46]. In order to explore the overall soil temperature change within the 20 cm plow layer under microwave irradiation, the temperature is analyzed in the whole cuboid in the soil model of Figure 25 (volume of 16 × 12 × 20 cm), and the average temperature in the area is defined as \bar{T}_α . The calculation method is shown in Equation (7). First, the soil temperature of each layer in different irradiation periods is averaged to obtain the average layer temperature \bar{T}_n . The $\bar{T}_1 \sim \bar{T}_{20}$ values were added and averaged to obtain the average soil temperature \bar{T}_α in the irradiated area of the cuboid. Figure 30 shows the average soil temperature T_a in the loess and black soil irradiation areas after microwave irradiation for 1~12 min, which is

positively correlated with the irradiation time. With the increase in soil moisture content, the average temperature \bar{T}_α of black soil decreases, that is, $\bar{T}_\alpha 10\% > \bar{T}_\alpha 15\% > \bar{T}_\alpha 20\% > \bar{T}_\alpha 23\%$. Figure 30 shows that the average temperature of some loess is therefore slightly higher than that of black soil when the moisture content is 15% and 20%. However, in most cases, the average temperature in the irradiated area of Northeast black soil is generally higher than that of North China loess, that is, $\bar{T}_\alpha \text{ black soil} > \bar{T}_\alpha \text{ loess}$.

$$\bar{T}_\alpha = (\bar{T}_1 + \bar{T}_2 + \bar{T}_3 + \dots + \bar{T}_{20}) / 20 \tag{7}$$

Table 4. The extreme points in the surface equation of the change in the internal temperature of the soil layer with irradiation time and soil depth.

	Soil Moisture Content	X (Irradiation Time)	Y (Soil Depth)	Z (\bar{T})
Loess	10%	12.54015	4.74245	92.11896
	15%	11.65806	5.58985	89.89108
	20%	10.56247	4.97283	87.11137
	23%	12.56472	2.66982	83.00965
Black soil	10%	12.39321	5.65879	97.55119
	15%	10.85128	5.6307	86.98526
	20%	10.81245	4.22685	84.56088
	23%	11.13109	3.59239	88.79240

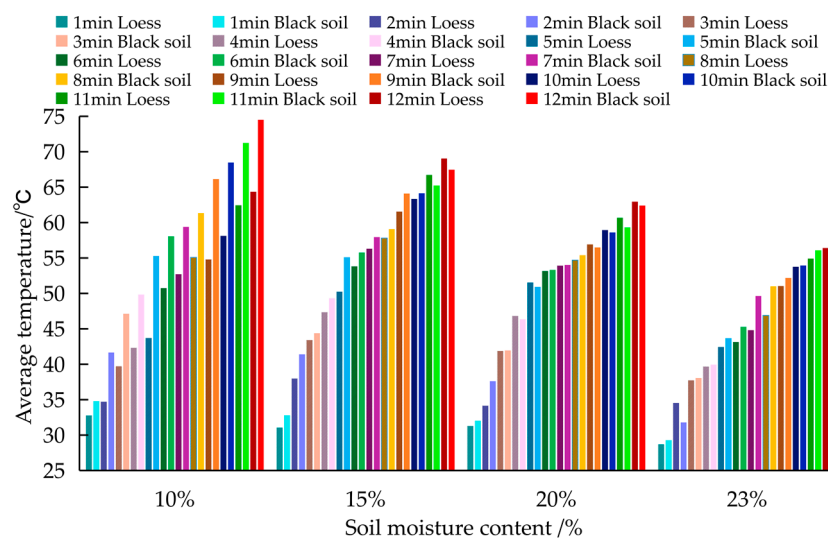


Figure 30. Average soil temperature (\bar{T}_α) in the microwave-irradiated area of the soil.

The microwave irradiation time and soil moisture content were used as independent variables, and the average soil temperature \bar{T}_α in the irradiation area was used as the dependent variable to draw a three-dimensional surface; the surface equation is shown in Table 5. Figure 31 shows the soil internal temperature when the moisture content of loess and black soil is 10%, 15%, 20% and 23% after microwave irradiation for 1~12 min. Among them, in the 12 min irradiation condition, the maximum temperature of loess in the microwave irradiation range is 69 °C (with a soil moisture content of 20%) and the average maximum temperature of black soil is 74 °C (with a soil moisture content of 10%) To explore the variation law of the internal temperature of the irradiated area of the soil with the irradiation time and soil moisture content, the three-dimensional surface given in Figure 31 was fitted, as shown in Figure 32; the corresponding fitting surface equation is given in Table 4. The temperature fitting surface of “irradiation time–soil depth” obtained above is the same as the temperature fitting surface of loess “irradiation time–soil water content”, which satisfies the same Gaussian mathematical model.

Table 5. Irradiation time–soil moisture content temperature surface equation.

Surface Fitting Equation (Loess)		Surface Fitting Equation (Black Soil)		
$\bar{T}_{\partial\text{loess}} = z_0 + A \exp\left\{-\frac{1}{2}\left(\frac{x-x_c}{\omega_1}\right)^2 - \frac{1}{2}\left(\frac{y-y_c}{\omega_2}\right)^2\right\}$		$\bar{T}_{\partial\text{black soil}} = z_0 + 0.25B\left[1 + \operatorname{erf}\left\{\frac{x-C}{\sqrt{2D}}\right\}\right]\left[1 + \operatorname{erf}\left\{\frac{y-E}{\sqrt{2F}}\right\}\right]$		
Parameters	z_0	-15.8487 ± 31.86192	z_0	-15.77101 ± 22.18914
	A	84.52756 ± 32.70872	B	90.89622 ± 23.03721
	x_c	14.4657 ± 1.64587	C	-0.6273 ± 2.0709
	ω_1	13.48069 ± 4.55263	D	6.97897 ± 1.22299
	y_c	0.15286 ± 0.00208	E	0.33741 ± 0.03576
	ω_2	0.14603 ± 0.03564	F	-0.11324 ± 0.02257
	R^2	0.97199	R^2	0.98244
\bar{T}_α	$\bar{T}_{\alpha\text{loess}15\%} >$ $\bar{T}_{\alpha\text{loess}20\%} >$ $\bar{T}_{\alpha\text{loess}10\%} >$ $\bar{T}_{\alpha\text{loess}23\%}$	\bar{T}_α	$\bar{T}_{\alpha\text{black soil}10\%} >$ $\bar{T}_{\alpha\text{black soil}15\%} >$ $\bar{T}_{\alpha\text{black soil}20\%} > \bar{T}_{\alpha\text{black soil}23\%}$	
$1 < x < 12, 0.1 < y < 0.23$				

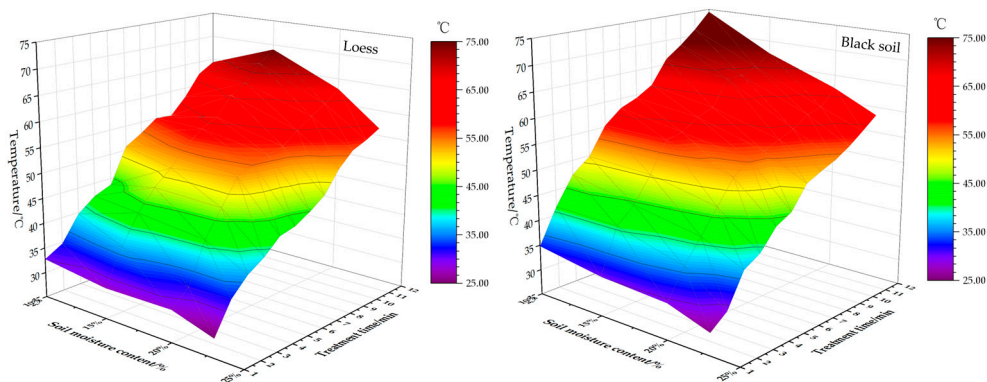


Figure 31. Variation in internal temperature in the soil irradiation area with irradiation time and soil moisture content.

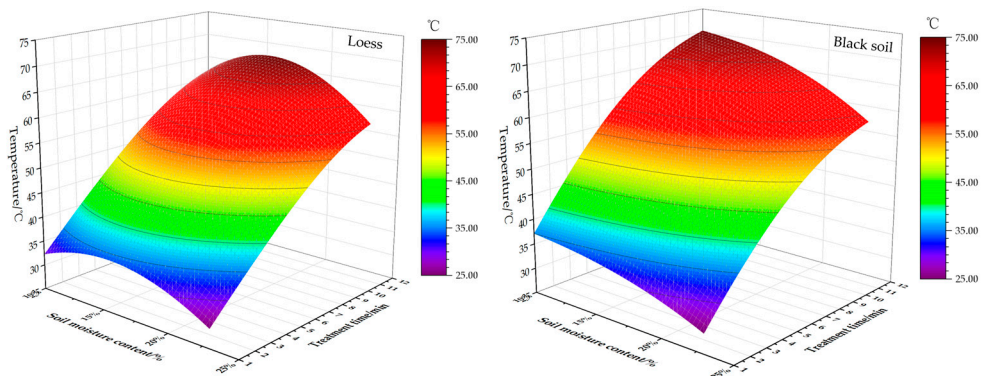


Figure 32. Fitting surface of the internal temperature of the soil irradiation area with the time of irradiation and soil moisture content (“irradiation time–soil moisture content” temperature surface).

In Figure 32, the maximum loess temperature in the three-dimensional fitting surface is 14.63%, 12, 67.28, and the black soil is 10%, 12, 70.35; that is, the loess in the curved surface obtained the maximum average soil temperature of 67.28 °C under 12 min microwave irradiation and a moisture content of 14.63%, and the black soil obtained the maximum average soil temperature of 70.5 °C under 12 min microwave irradiation and

10% moisture content. According to the change in the internal temperature of the loess fitting surface with the soil moisture content in Figure 32, the law can be drawn as follows: $\bar{T}_{\alpha 15\%} > \bar{T}_{\alpha 20\%} > \bar{T}_{\alpha 10\%} > \bar{T}_{\alpha 23\%}$. This also confirms the abovementioned relationship of the internal temperature of black soil with soil moisture content accuracy. Taking the soil temperature (Z axis) as a reference and comparing the temperature fitting surfaces of black soil and loess in Figure 32, it can be concluded that the temperature fitting surface of black soil is above the loess, that is, the average temperature of black soil is generally higher than that of loess. According to the obtained “irradiation time–soil depth” temperature fitting equation of North China loess and Northeast black soil, the soil temperature \bar{T}_{α} after microwave irradiation for any period of time within the conventional water content range can be obtained to analyze the soil temperature of microwave soil under different working conditions.

Large populations of soil pests, phytopathogenic fungi, and bacteria can reach inactivation conditions at 60 °C. When the temperature surpasses 71 °C, all plant pathogenic fungi and bacteria can be killed, which also includes most plant viruses; the inactivation conditions of grass seeds are relatively high (80 °C) [47]. In a study of the microwave inactivation of *Echinochloa crus. galli* (L.) P. Beauv., a problematic weed in global rice regions, increasing soil temperature to 79.6 °C reduced its germination rate by 80–100% [48]. In general, 5 min of microwave irradiation can cause a high temperature of 92 °C to be reached [49], which is very similar to the test point temperature of 93.7 °C (10% black soil, 4 cm) obtained in this paper for 5 min. With increasing irradiation time, the soil temperature also increases. The microwave system with a power of 4 kW applied in agricultural microwave soil disinfection can cause the soil temperature to exceed 100 °C within an irradiation time of 15 min [50]. In this study, the maximum temperature of the 6 min irradiation test point was 100.5 °C (10% black soil, 4 cm), but this only represents the local temperature around the test point. When the irradiation time reached 12 min, the maximum temperature of the soil layer was 100.04 °C (10% black soil, the average temperature within the 4 cm depth irradiation range), and the average temperature \bar{T}_{α} within the 20 cm depth range was 74 °C (10% black soil). All plant pathogenic fungi and bacteria in the soil were killed. In field production, the most suitable soil depth for the germination of most weed seeds is 1–4 cm, and the germination of grass seeds is extremely low when the soil depth exceeds 6 cm [51]. In the test, 12 min irradiation conditions can kill grass seeds with a soil depth of more than 10 cm, which also confirms the feasibility and effectiveness of microwave irradiation in soil disinfection. When microwave units are installed in large soil disinfection equipment, the number of microwave units is generally matched according to the power of the power system, and they are placed in an orderly manner to ensure the adequacy of microwave soil disinfection [52].

Long-Term Microwave Action Soil Irradiation Depth Test Results

In the test, the depth at which the loess was clearly dry was 9.5 cm, and for the black soil it was 9 cm. Under the same irradiation conditions, the observed drying depths of loess and black soil at 20% soil moisture content are 7 and 7.5 cm, respectively, as shown in Figure 33. This does not, however, represent the working depth that can only be achieved by microwave irradiation. The drying depth of the soil after microwave irradiation directly reflects the influence of the soil moisture content on the soil internal temperature. Figures 34 and 35 show the visible drying depth of the soil after microwave irradiation for 1–12 min. When the microwave irradiation time is the same, the visible irradiation depth of loess and black soil satisfies $\text{Depth}_{23\%} < \text{Depth}_{20\%} < \text{Depth}_{15\%} < \text{Depth}_{10\%}$. The difference in drying depth between loess and black soil under the same experimental conditions is mainly caused by the differences in soil composition and thermal conductivity.

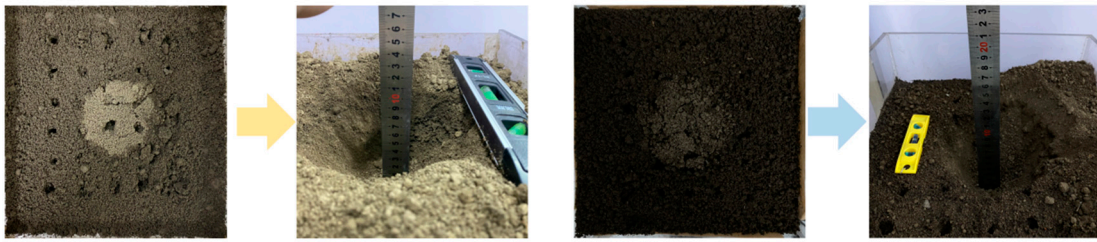


Figure 33. Soil surface and visible drying depth of 20% water-bearing loess and black soil after 12 min of microwave irradiation.

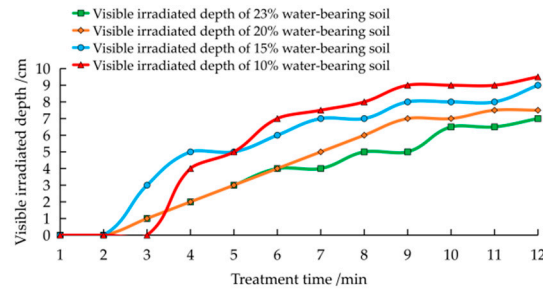


Figure 34. Visible drying depth of North China loess.

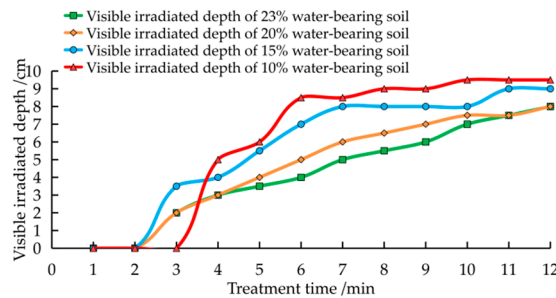


Figure 35. Visible drying depth of Northeast black soil.

The unique penetrability of microwaves causes the maximum temperature of the soil after irradiation to appear at a depth of several centimeters from the soil surface. The location of the maximum temperature in the microwave soil irradiation test mainly depends on the soil moisture content. Figures 36 and 37 show the depths of the maximum temperature test points of loess and black soil in the soil model under 10%, 15%, 20% and 23% moisture content. The maximum temperature points of loess under four moisture contents are 3.8, 3.5, 3.3 and 2.4 cm away from the soil surface, respectively, and the maximum temperature points of black soil are 3.6, 3.1, 2.6 and 2.2 cm (average depth). With the increase in soil moisture content, the highest temperature point collected under the same irradiation time became closer to the soil surface.

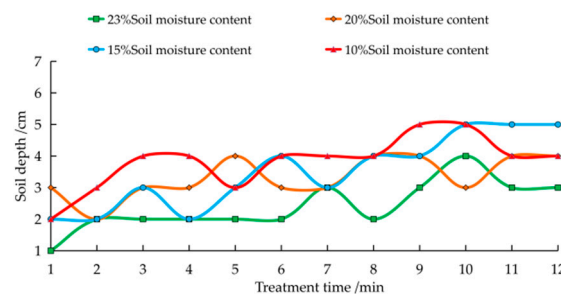


Figure 36. The maximum temperature \bar{T}_{max} of the loess internal test point.

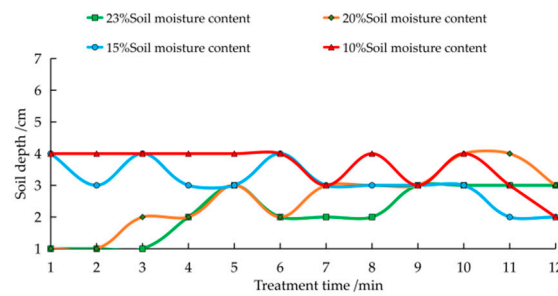


Figure 37. The maximum temperature $\bar{T}_{n\max}$ of the black soil internal test point.

Figures 38 and 39 show the average maximum temperature $\bar{T}_{n\max}$ of the loess and black soil layers at the soil depth. The same rule is satisfied: as the soil moisture content increases, the location of the maximum temperature approaches the soil surface. When the soil moisture content was 10%, 15%, 20%, and 23%, the average maximum temperature $\bar{T}_{n\max}$ of the loess layer after microwave irradiation appeared at 3.9, 3.6, 3.3, and 2.4 cm below the soil surface, and in the black soil it appeared at 4.0, 3.3, 2.75, and 2.3 cm, respectively. The position of the maximum temperature $\bar{T}_{n\max}$ of the test point is similar to the position of the average maximum temperature $\bar{T}_{n\max}$ of the soil layer. Therefore, the treatment range determined in this paper is in line with the law of microwave soil heating. Compared with the short-term 10~60 s microwave irradiation test, the maximum temperature of loess with 10% and 20% water content appeared at 3.5 cm and 2.16 cm from the soil surface, respectively. The depth was slightly smaller than that of the long-term microwave irradiation under the same water content, which was mainly the result of the long-term microwave irradiation and soil heat conduction [53].

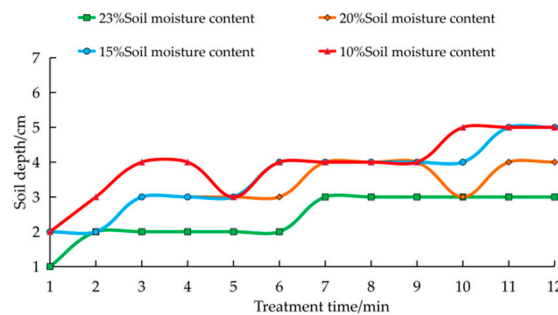


Figure 38. The location of the average maximum temperature $\bar{T}_{n\max}$ of the loess layer.

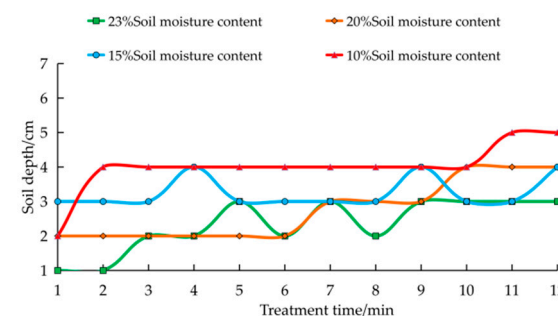


Figure 39. The location of the average maximum temperature $\bar{T}_{n\max}$ of the black soil layer.

After 1~12 min of microwave soil irradiation, the soil in the irradiation range absorbs energy, and the water evaporates. With increasing irradiation time, the depth of the soil gradually dries, and the color is clearly lighter than that of the normal water-bearing soil. After 1~12 min of microwave soil irradiation, the soil in the irradiation range absorbs energy, and the water evaporates. As the irradiation time increased, the deeper soil gradually dried. Compared with normal water-bearing soil, the color is clearly lighter. The overall dry area

of the soil presents an inverted cone shape. This is the result of microwave action and soil heat conduction, which is consistent with the soil model temperature simulation results presented in this paper. The skin effect is unavoidable in the process of microwave soil disinfection, so the penetrability of microwaves is not infinite, resulting in a maximum temperature value in the soil under the action of microwaves, which often appears a few centimeters below the surface [54]. The penetration degree of microwaves during soil irradiation depends on the soil loss factor ϵ'' , which can be expressed by Equation (8) as:

$$\epsilon = \epsilon' - j\epsilon'' \quad (8)$$

where ϵ is the complex permittivity, ϵ' is the permittivity, ϵ'' is the dielectric loss factor, and the value of j is $\sqrt{-1}$.

In the process of microwave soil irradiation, the greater the loss factor of the soil, the greater the conversion of microwave energy to heat energy, and the shallower the soil depth [55,56]. The values of the dielectric properties of soil can vary depending on factors such as frequency, water content, density, and temperature [57–59]. When the soil water content is the only variable, the loss factor ϵ'' increases as the soil water content increases, and it becomes more difficult for microwaves to act at greater depths inside the soil. When 10~23% water-bearing soil is irradiated by microwaves for 1~12 min, the evaporation quality of the soil water is between 17 and 135 g, and approximately 10 g of water is lost per min of microwave irradiation on average. The dissipation of water leads to a slight decrease in the soil loss factor ϵ'' , but it is beneficial to the penetration of microwaves for soil disinfection operations [60]. For microwaves in the frequency range of 0.9 to 3 GHz, the dielectric parameter ϵ' of soil can be considered constant in agricultural production. The variability of the complex permittivity ϵ in the studied frequency range is much lower than the various factors considered, and the effect of soil drying during irradiation is generally negligible [61].

4. Conclusions

In the experimental study of microwave irradiation on the soil surface, given the same soil moisture content and microwave irradiation time, the surface temperature of black soil irradiated by microwaves is higher than that of loess, and the soil surface temperature and moisture content have a positive correlation. Among them, the soil moisture content, microwave irradiation time and soil type are the main factors affecting the microwave soil heating law. The experiment first explores the heating law of the soil surface. Due to the evaporation of soil moisture during the irradiation process, the soil surface under the waveguide presents a circular area. As the irradiation time increases, the diameter of the circular area approaches the long side of the rectangular waveguide port. The thermal map collected by the infrared sensor and the soil surface temperature map in the simulation also reflect the same law. The relationship between the diameter (R) of the irradiated area on the soil surface and the soil moisture content is $R_{\text{surface}23\%} > R_{\text{surface}20\%} > R_{\text{surface}15\%} > R_{\text{surface}10\%}$. The surface temperature law of North China loess and Northeast black soil is $T_{\text{surface}23\%} > T_{\text{surface}20\%} > T_{\text{surface}15\%} > T_{\text{surface}10\%}$. The maximum soil surface temperature of black soil was higher than that of loess at the four soil moisture contents. Using the PT100 temperature sensor matrix to obtain the soil temperature of the 20 cm plow layer, it was found that the highest temperature induced by microwaves in the soil occurs inside the soil, not on the surface. The unique penetration of microwaves makes the highest temperature of the soil test point often appear 3~4 cm away from the soil surface. The internal temperature value of the soil is proportional to the irradiation time. When the microwave irradiation time is the same, the relationship between the soil depth at which the maximum temperature value of the loess and black soil occurs and the soil moisture content is: $\text{Depth}_{23\%} < \text{Depth}_{20\%} < \text{Depth}_{15\%} < \text{Depth}_{10\%}$. As the soil moisture content increases, the maximum temperature of the soil approaches the soil surface. Combined with the simulation results and the change in soil internal temperature in each irradiation time period, the central cube area of $160 \times 120 \text{ mm} \times 20 \text{ mm}$ was determined as the

effective operating range of the microwave unit. As stated, it is not comprehensive to study only the highest temperature obtained by the sensor in microwave soil disinfection. In this paper, the method of stratification in the microwave effective operating range is used to analyze the average temperature \bar{T}_n of the layer, and it is found that the position of the maximum temperature $\bar{T}_{n \max}$ of the layer is very similar to the position of the maximum temperature $\bar{T}_{n \max}$ of the test point. Through the fitted temperature surface of “irradiation time–soil depth”, the average temperature T_n at each depth in the 20 cm cultivated layer of North China loess and Northeast black soil can be obtained after 1~12 min of microwave irradiation. The effectiveness of soil disinfection is generally measured by its lethality for soil pathogens, harmful insects and grass seeds. The average temperature of the 20 cm deep soil irradiation area is \bar{T}_α . In the 12 min microwave soil irradiation test, the maximum temperature reached for loess is 69 °C, obtained in soil with a moisture content of 20%; the temperature of black soil is 74 °C, obtained in soil with a moisture content of 10%. The “irradiation time–soil moisture content” temperature surface is fitted, and the extreme point of the surface shows that the soil moisture content when the average temperature of the irradiation area reaches the maximum value is 14.63% (loess) and 10% (black soil). The variation law of the average temperature T_α in the irradiation area with the soil moisture content is: $\bar{T}_{\alpha 15\%} > \bar{T}_{\alpha 20\%} > \bar{T}_{\alpha 10\%} > \bar{T}_{\alpha 23\%}$ (loess); $\bar{T}_{\alpha 10\%} > \bar{T}_{\alpha 15\%} > \bar{T}_{\alpha 20\%} > \bar{T}_{\alpha 23\%}$ (black soil). When the microwave irradiation conditions are the same, it generally satisfies: $\bar{T}_{\alpha \text{ black soil}} > \bar{T}_{\alpha \text{ loess}}$. According to the temperature surface equation of “irradiation time–soil moisture content”, the average temperature \bar{T}_α in the irradiation area under the conventional moisture content of North China loess and Northeast black soil under microwave irradiation can be obtained, which can be used for diseases, insects and weeds in the process of microwave soil disinfection. Inactivation conditions provide some reference.

Author Contributions: Conceptualization, C.Z. (Chunjiang Zhao) and X.S.; Methodology, X.S., C.Z. (Changyuan Zhai), S.Y. and C.Z. (Chunjiang Zhao); Validation, S.Y.; Formal analyses, S.Y. and H.M.; Investigation, X.S., H.M.; Resources, C.Z. (Chunjiang Zhao), C.Z. (Changyuan Zhai); Data curation, X.S.; Writing—original draft, X.S.; Writing—review and editing, C.Z. (Chunjiang Zhao), C.Z. (Changyuan Zhai) and S.Y.; Funding acquisition, C.Z. (Chunjiang Zhao), C.Z. (Changyuan Zhai); Supervision, C.Z. (Chunjiang Zhao) and C.Z. (Changyuan Zhai). All authors have read and agreed to the published version of the manuscript.

Funding: The support was provided by (1) the Special Project on Capacity Building of Scientific and Technological Innovation of Beijing Academy of Agriculture and Forestry Sciences (KJ CX20210402); (2) Key R&D Projects in Hebei Province (V1623741033097); and (3) Outstanding Scientist Program of Beijing Academy of Agriculture and Forestry Sciences (JKZX202212).

Institutional Review Board Statement: Not applicable.

Informed Consent Statement: Not applicable.

Data Availability Statement: The data presented in this study are available on request from the corresponding author.

Conflicts of Interest: The authors declare no conflict of interest.

References

- Du, Y. Research on the status and role of facility agriculture in ecological environment construction. *New Agric.* **2022**, *5*, 42.
- Cao, A.; Fang, W.; Li, Y.; Yan, D.; Wang, Q.; Guo, M.; Huang, B.; Song, Z.; Jin, Q. Review of 60 years of soil fumigation and disinfection in my country. *J. Plant Prot.* **2022**, *49*, 325–335. [[CrossRef](#)]
- Liu, Z.; Zhong, H.; Li, Y.; Wen, Q.; Liu, X.; Jian, Y. Characteristics of China’s grain production changes in the past 20 years and its impact on regional grain supply and demand patterns. *J. Nat. Resour.* **2021**, *36*, 1413–1425. [[CrossRef](#)]
- Fang, W.; Cao, A.; Wang, Q.; Yan, D.; Li, Y.; Jin, X.; Zhao, Q.; Qiu, Y.; Zhao, H. A new integrated soil disinfection machine improves the uniformity of dazomet in soil. *Sci. Agric. Sin.* **2021**, *54*, 2570–2580. [[CrossRef](#)]
- Wang, Q.; Yan, D.; Wang, X.; Li, X.; Cao, A. Research advances in soil fumigants. *J. Plant Prot.* **2017**, *44*, 529–543.
- Wang, X.-N.; Cao, A.-C.; Yan, D.-D.; Wang, Q.; Huang, B.; Zhu, J.-H.; Wang, Q.-X.; Li, Y.; Ouyang, C.-B.; Guo, M.-X.; et al. Evaluation of soil flame disinfestation (SFD) for controlling weeds, nematodes and fungi. *J. Integr. Agric.* **2020**, *19*, 164–172. [[CrossRef](#)]

7. Hess, M.C.M.; Buisson, E.; Mesléard, F. Soil compaction enhances the impact of microwave heating on seedling emergence. *Flora* **2019**, *259*, 151457. [[CrossRef](#)]
8. Tang, T.; Liu, Y.; Wen, G.; Liu, G.; Wen, J.G.; Liu, L. Simulation for propagation of high-power microwave with repeated monopulses in soil. *IEEE Antennas Wirel. Propag. Lett.* **2019**, *18*, 1308–1311. [[CrossRef](#)]
9. Rahi, G.S.; Rich, J.R. Effect of moisture on efficiency of microwaves to control plant-parasitic nematodes in soil. *J. Microw. Power Electromagn. Energy* **2011**, *45*, 86–93. [[CrossRef](#)]
10. Sabry, A.; Allam, A.; Abdel-Rahman, A.B.; El-Ansary, D. A novel microwave applicator for sandy soil disinfection. In Proceedings of the 2018 Progress in Electromagnetics Research Symposium (PIERS-Toyama), Toyama, Japan, 1–4 August 2018; IEEE: New York, NY, USA, 2018; pp. 636–641.
11. Bebawi, F.; Cooper, A.P.; Brodie, G.; Madigan, B.A.; Vitelli, J.; Worsley, K.J.; Davis, K. Effect of microwave radiation on seed mortality of rubber vine (*Cryptostegia grandiflora* R.Br.), parthenium (*Parthenium hysterophorous* L.) and bellyache bush (*Jatropha gossypifolia* L.). *Plant Prot. Q.* **2007**, *22*, 136–142.
12. Brodie, G.; Pasma, L.; Bennett, H.; Harris, G.; Woodworth, J. Evaluation of microwave soil pasteurization for controlling germination of perennial ryegrass (*Lolium perenne*) seeds. *Plant Prot. Q.* **2007**, *22*, 150–154.
13. Liu, H.J.; Wang, P.F.; Li, J.P.; Yang, X. Research on weed pre-emergent control using microwave radiation. *J. Chin. Agric. Mech.* **2019**, *40*, 59–62.
14. Sun, L.; Yu, F.; Ge, X. Experimental study on the application of self-propelled fine-rotating soil flame insecticide in facility vegetable production. *Jiangsu Agric. Mech.* **2020**, *4*, 4.
15. Bisceglia, B. Innovative applications in horticulture: Electromagnetic fields treatment of soil and seeds. *Acta Hort.* **2017**, *1164*, 85–92. [[CrossRef](#)]
16. Gai, Z.; Sun, L.; Wei, D.; Wang, C.L.; Yang, G.J.; Lin, Z.Y. Effects of microwave on soil microorganisms and functional diversity of their communities. *Henan Agric. Sci.* **2007**, *3*, 5.
17. O'Brien, M. *Microwave—A Fresh Look at Old Technology for Weed Control*; The Australian Cottongrower: Toowoomba, Australia, 2017; pp. 26–28.
18. Wang, Z.; Shi, Y.; Liu, C. Control effect of microwave disinfection on pathogenic microorganisms in soil. *Henan Agric. Sci.* **2010**, *12*, 3.
19. Maddalwar, S.; Nayak, K.K.; Kumar, M.; Singh, L. Plant microbial fuel cell: Opportunities, challenges, and prospects. *Bioresour. Technol.* **2021**, *341*, 125772. [[CrossRef](#)]
20. Zhou, Z.; Bu, X.; Wu, Y.; Xue, J.H. Effects of biochar on soil microbial properties. *J. Nanjing For. Univ. Nat. Sci.* **2016**, *40*, 8.
21. Gai, Z.; Zhou, Y.; Wang, B.; Li, D.W.; Guo, X.G.; Wei, X.D. Soil test study of microwave disinfection facility. *South. Agric. J.* **2007**, *38*, 174–176.
22. Wang, C.; Cai, G.; Liu, X.; Wu, M. Prediction of soil thermal conductivity based on Intelligent computing model. *Heat Mass Transf.* **2022**. [[CrossRef](#)]
23. Brodie, G.; Hamilton, S.; Woodworth, J. An assessment of microwave soil pasteurization for killing seeds and weeds. *Plant Prot. Q.* **2007**, *22*, 143–149.
24. Khan, M.J.; Brodie, G.I.; Gupta, D. Microwave: A novel approach to tackle herbicide resistance in no-till farming systems. In Proceedings of the 21st Australasian Weeds Conference, New South Wales, Australia, 9–12 September 2018; Johnson, S., Weston, L., Wu, H.W., Auld, B., Eds.; CABI: Wallingford, UK, 2019; pp. 140–143.
25. Fanti, A.; Spanu, M.; Lodi, M.B.; Desogus, F.; Mazzarella, G. Nonlinear analysis of soil microwave heating: Application to agricultural soils disinfection. *IEEE J. Multiscale Multiphys. Comput. Tech.* **2017**, *2*, 105–114. [[CrossRef](#)]
26. Nelson, S.O. A review and assessment of microwave energy for soil treatment to control pests. *Trans. ASAE* **1996**, *39*, 281–289. [[CrossRef](#)]
27. Kim, J.; Mun, S.C.; Ko, H.-U.; Kim, K.-B.; Khondoker, M.A.H.; Zhai, L. Review of microwave assisted manufacturing technologies. *Int. J. Precis. Eng. Manuf.* **2012**, *13*, 2263–2272. [[CrossRef](#)]
28. Rahi, G.; Rich, J. Potential of microwaves to control plant-parasitic nematodes in soil. *J. Microw. Power Electromagn. Energy* **2007**, *42*, 5–12. [[CrossRef](#)]
29. Li, Y. Plug-in Microwave Soil Sterilization and Insecticide Device. Patent CN2607780, 31 March 2004.
30. Nelson, S.O.; Kraszewski, A.W. Dielectric properties of materials and measurement techniques. *Dry. Technol.* **1990**, *8*, 1123–1142. [[CrossRef](#)]
31. Zhou, M.C. Study on Numerical Simulation of Microwave Heating and Temperature Control. Ph.D Thesis, Southwest University of Science and Technology, Mianyang, China, 2020; pp. 13–14.
32. Mironov, V.L.; Bobrov, P.P.; Fomin, S.V.; Karavaiskii, A.Y. Generalized refractive mixing dielectric model of moist soils considering ionic relaxation of soil water. *Russ. Phys. J.* **2013**, *56*, 319–324. [[CrossRef](#)]
33. Behzadi, M.; Dayyari, S.; Ali Akbarian, H.; Nezamabadi, N. Design and fabrication of a microwave weed killer device for weed control applications. *Int. J. Eng.* **2019**, *32*, 947–953.
34. Jeong, C.H.; Seo, D.G.; Lee, W.S. Improved Heating Uniformity of a 3-kWatt 2.45 GHz Microwave Dryer Using Multiple Multi-Slotted Waveguides. In Proceedings of the 2019 International Applied Computational Electromagnetics Society Symposium (ACES), Miami, FL, USA, 14–19 April 2019; pp. 1–2.

35. Brodie, G.; Harris, G.; Pasma, L.; Travers, A.; Leyson, D.; Lancaster, C.; Woodworth, J. Microwave soil heating for controlling ryegrass seed germination. *Trans. ASABE* **2009**, *52*, 295–302. [[CrossRef](#)]
36. Metaxas, A.C.; Meredith, R.J. *Industrial Microwave Heating*; IEEE Power Engineering Series 4; Peter Peregrinus Ltd.: London, UK, 1993.
37. Zhang, F.; Wang, X.; Liang, X.; Kong, X.; Zhang, Q.; Yang, L. Discrimination and analysis of soil classes and subclasses and their survey mapping in the second national soil census. *Soil* **2014**, *46*, 761–765. [[CrossRef](#)]
38. Chang, Y. Spatial Distribution Characteristics and Driving Factors of Soil Microorganisms in Long-Term Maize Continuous Cropping in Jilin Province. Ph.D Thesis, Jilin Agricultural University, Jilin, China, 2021; pp. 2–3.
39. Li, T. Relationship between geochemical process and element background content in Beijing soil. *Environ. Sci.* **1987**, *4*, 59–63.
40. Liu, Z.; Gao, Y.; Liu, Z.; Duan, A. Effects of rainfall characteristics and mulching patterns on soil moisture in wheat fields. *Trans. Chin. Soc. Agric. Eng.* **2012**, *28*, 113–120.
41. Wang, Z.; Liu, Z.; Cao, Z.; Li, Y.; Zhang, Z.; Wang, L. Effects of biochar on water-holding properties of black soil in Northeast China. *Chin. J. Agric. Eng.* **2019**, *35*, 147–153.
42. Wei, H.; Meng, F. Research on soil conductivity measurement based on four-terminal method and time-domain reflectometry. *J. Agric. Mach.* **2019**, *50*, 237–242.
43. Han, C.; Yang, W.; Dou, H.; Wang, X.; Hu, L.; Zhai, C. Design and test of a rapid detection system for soil conductivity in the field. *J. Agric. Mach.* **2022**, *53*, 301–310.
44. Ciccattelli, A.; Guarino, F.; Castiglione, S.; Luca, A.D.; Esposito, D.; Grimaldi, M.; Bisceglia, B. Microwave treatment of agricultural soil samples. In Proceedings of the 2015 IEEE 15th Mediterranean Microwave Symposium (MMS), Lecce, Italy, 30 November–2 December 2015; IEEE: New York, NY, USA, 2015; pp. 1–3.
45. Wang, M.; Xiao, H.; Song, W.D.; Zhu, T.; Zhao, R.; Xiao, S.W. Effects of microwave treatment on root-knot nematodes in greenhouse continuous cropping soils. *Chin. J. Agric. Mech.* **2013**, *2013*, 95–99.
46. Li, Y.; Cao, H.; Xu, F.; Ren, W.; Liu, J.; Zhang, S.; Zhang, F.; Chen, Z. Effects of different forms of soil disinfection on soil physical properties and cucumber growth. *Chin. J. Eco-Agric.* **2010**, *18*, 1189–1193. [[CrossRef](#)]
47. Brodie, G.; Ryan, C.; Lancaster, C. Microwave technologies as part of an integrated weed management strategy: A review. *Int. J. Agron.* **2012**, *2012*, 636905. [[CrossRef](#)]
48. Vidotto, F.; De Palo, F.; Ferrero, A. Effect of short-duration high temperatures on weed seed germination. *Ann. Appl. Biol.* **2013**, *163*, 454–465. [[CrossRef](#)]
49. Ma, S.; Jin, H.; Zhao, Y.; Hu, H.; Hu, X. Establishment of microwave heating soil simulation model and its weeding and disinfection effect. *J. Northwest A&F Univ.(Nat. Sci. Ed.)* **2022**, *8*, 1–9. [[CrossRef](#)]
50. Velázquez-Martí, B.; Gracia-López, C. Thermal effects of microwave energy in agricultural soil radiation. *Int. J. Infrared Millim. Waves* **2004**, *25*, 1109–1122. [[CrossRef](#)]
51. Cao, D.; Dai, W.; Qiang, S.; Song, X. Effects of different soil and water depths on the emergence of 15 weedy rice populations in China. *Jiangsu Agric. J.* **2011**, *27*, 750–755.
52. Joines, W.T. Microwave System and Method for Controlling the Sterilization and Infestation of Crop Soils. Patent US20090232602A1, 19 April 2012.
53. Sun, X.; Zhai, C.; Yang, S.; Ma, H.; Zhao, C. Simulations and experiments of the soil temperature distribution after 2.45-GHz short-time term microwave treatment. *Agriculture* **2021**, *11*, 933. [[CrossRef](#)]
54. Paolanti, M.; Pollini, R.; Frontoni, E.; Mancini, A.; Leo, R.D.; Zingaretti, P.; Bisceglia, B. Exposure protocol setup for agro food treatment. Method and system for developing an application for heating in reverberation chamber. In Proceedings of the 2015 IEEE 15th Mediterranean Microwave Symposium (MMS), Lecce, Italy, 30 November–2 December 2015; IEEE: New York, NY, USA, 2015; pp. 1–4.
55. Hoekstra, P.; Delaney, A. Dielectric properties of soils at UHF and microwave frequencies. *J. Geophys. Res. (1896–1977)* **1974**, *79*, 1699–1708. [[CrossRef](#)]
56. Janney, M.A.; Kimrey, H.D. Diffusion controlled processes in microwave-fired oxide ceramics. In *Proceedings of the MRS Symposium*; Snyder, W.B., Sutton, W.H., Eds.; Microwave Processing of Materials: Washington, DC, USA, 1991; pp. 215–227.
57. Davis, F.S.; Wayland, J.R.; Merkle, M.G. Ultrahigh-frequency electromagnetic fields for weed control: Phytotoxicity and selectivity. *Science* **1971**, *173*, 535–537. [[CrossRef](#)]
58. Olsen, R.G. A Theoretical investigation of microwave irradiation of seeds in soil. *J. Microw. Power* **1975**, *10*, 281–296. [[CrossRef](#)]
59. Giovannini, C.; Lucchesi, S.; Giachetti, M. Effects of heating on some chemical parameters related to soil fertility and plant growth. *Soil Sci.* **1990**, *149*, 334–350. [[CrossRef](#)]
60. Lin, Z.; Sui, L.; Zheng, X.; Li, B.; Zou, L.; Liu, C. Influence of microwave foam drying on the dielectric properties of raspberry fruit powder. *Food Mach.* **2014**, *30*, 10–14+309. [[CrossRef](#)]
61. Velázquez-Martí, B.; Gracia-López, C.; Plaza-Gonzalez, P.J. Determination of dielectric properties of agricultural soil. *Biosyst. Eng.* **2005**, *91*, 119–125. [[CrossRef](#)]